

# About the convergence of scaling field expansions between two RG fixed points

Y. Meurice and S. Niermann

*Department of Physics and Astronomy, The University of Iowa, Iowa City, Iowa 52242, USA*

We propose to combine the scaling fields associated with the high-temperature fixed point with those associated with the unstable fixed point in order to calculate the magnetic susceptibility or higher derivatives of the free energy. The method relies on the estimation of RG invariant quantities constructed out of the two types of scaling fields and we need accurate expansions in overlapping domains. We construct explicit series in two examples (Dyson's hierarchical model and a simplified version of it). We provide numerical evidence that the expansions of the scaling fields associated with the two fixed points scale accurately in overlapping domains. We explain how an extension of this strategy can lead to complete analytical expressions for all the thermodynamical quantities.

**Keywords:** Renormalization group, scaling fields, high-temperature expansion, hierarchical model, normal forms.

**PACS:** 05.50.+q, 11.10.Hi, 64.60.Ak, 75.40.Cx

## I. INTRODUCTION, MOTIVATIONS AND MAIN RESULTS

### A. About the local existence of the scaling fields

A common strategy in problems involving nonlinear flows near a singular point, is to construct a new system of coordinates for which the governing equations become linear. This theme appears in various parts of Poincaré’s work, starting with his dissertation. It also permeates through Arnold’s book [1] on geometrical methods applied to differential equations. In the following, we use the generic expression “the normal form method”, to qualify these reductions to linear normal form. It seems intuitively clear that if the original problem is sufficiently nontrivial, the normal form method can only work in some limited way, locally, because the flows of the nonlinear problem have global properties which do not match those of the linear flows. Understanding these limitations is often an interesting way to approach dynamical systems with a complex behavior.

A well-known argument for the inadequacy of such procedure (which extends beyond the special case of an expansion near a singular point discussed above) was provided by Poincaré [2] in the context of perturbed integrable Hamiltonians. He discovered that even though it is possible to write a formal perturbative series for the action-angle variables, some coefficients have “small denominators”, and generically, the series are ill-defined. However, under some restrictions (formulated according to some appropriate version of the KAM theorem [1]), perturbation theory can still provide interesting information. In particular it can be used as a guide to understand the onset of chaos in numerical experiments. More generally, whenever small denominators (also called resonances) can be avoided or controlled, some local expansion seems possible.

Almost thirty years ago, Wegner [3], introduced quantities that transformed multiplicatively under a RG transformation. He called them “scaling fields” and we will use his terminology in the following. These fields play a central role in the presentation of the basic ideas of the Renormalization group (RG) and in the parametrization of the thermodynamical

quantities such as the magnetization or the magnetic susceptibility. They appear in almost any review on the subject (see for instance Ref. [4]). As in the case of Hamiltonian dynamics, there exists a formal series expansion for the scaling variables (see Eq. (4.9) in Ref. [3]). It is commonly assumed that the functions defined with this procedure are analytic, at least within a certain neighborhood of the fixed point. However, for most non-trivial models, it is very difficult to prove this assumption. In particular, it is difficult to address the question of small denominators because it requires an accurate calculation of the eigenvalues of the linearized RG transformation.

If it is nevertheless the case that the small denominator problem can be controlled and that some expansion is well-defined locally, there remain several important questions. What is the domain of convergence of this expansion? How does the accuracy of an expansion with a finite number of terms evolve when we move away from the fixed point? Again there are practical difficulties to answer these questions. The first one is that the exact form of the RG transformation is usually unknown. The second difficulty is that the number of coefficients to be determined in these expansions increases very rapidly with the non-linearity order when several scaling fields are taken into account. Given the central role played by the scaling fields, we think that it is important to address these convergence issues. Before we start discussing model calculations, we would like to extend our local point of view (the neighborhood of a fixed point) to a global one.

## B. Global issues and general objectives

If the small denominators can be controlled and if an expansion of the scaling fields converge within some neighborhood of the fixed point, it is unclear how the information regarding the RG flows outside of the domain of convergence can be incorporated in a calculation of the thermodynamical quantities. More practically, if we have at hand an expansion *with a finite number of terms* that has a desired accuracy within some smaller neighborhood of the fixed point, what should we do when the flows leave this domain of

validity?

The point of view that we want to advocate here is that one should combine different sets of scaling fields. Even though the scaling fields are almost always constructed in the vicinity of Wilson's fixed point, they can in principle be constructed near any other fixed point. If one can find some overlap among the domains of convergence of these expansion it is in principle possible to reconstruct the flows, given their initial values. In other words, we would like to develop a new analytical approach to complement the existing methods used to deal with the crossover between fixed points, namely, the Monte Carlo method [5–7], a combination of field-theoretical methods and mean field calculations [8–12] or the study of the entropy associated with the RG flows [13].

We want to discuss some aspects of this idea in the case of spin models having a nontrivial unstable fixed point. Our general goal is to solve such models (e.g., to provide accurate analytical formulas for the thermodynamical quantities) in the symmetric phase by constructing the scaling fields near the three relevant fixed points: the Gaussian fixed point, Wilson's fixed point and the high-temperature (HT) fixed point. The idea is represented schematically in Fig. 1.

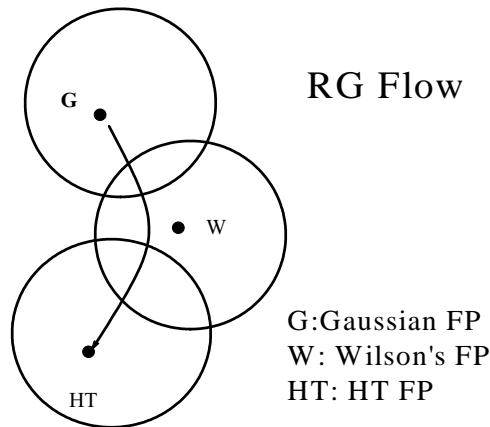


FIG. 1. Schematic representation of a RG flow starting near the Gaussian fixed point, passing near Wilson's fixed point and ending at the stable high-temperature fixed point. The circles represent the domains of validity of expansions of the scaling fields near the three fixed points.

### C. The scope of this investigation

In the following, our investigation will be limited to the high-temperature (HT) phase of spin models. We will consider the flows starting in the neighborhood of Wilson's fixed point and ending at the HT fixed point. We will mostly concentrate on the flows from the unstable fixed point to the HT fixed *starting along the unstable direction*. With this restriction, the initial values of the flow will be restricted to one (relevant) direction. The perturbative inclusion of the irrelevant directions will only be briefly discussed. On the other hand, when the flows move away from Wilson's fixed point, they are not in any particular directions with respect to the HT fixed point and a full multivariable approach is necessary. This is a difficult nonlinear problem for which a satisfactory treatment will be provided in a specific case.

The main goal of this article is to discuss the large order behavior of the expansions of the scaling fields with empirical examples. Our approach is numerical. All the statements regarding the convergence of the expansions will be based on the analysis of the empirical series with well-established estimators [14]. No attempt is made to prove these statements rigorously.

Despite the existence of increasingly sophisticated methods used for various expansions in nearest neighbor models (see e.g., Ref. [15]), it is still a major time investment to learn about the large order behavior of these expansions. In order to test the general ideas, we have considered approximations for which the large order can be reached more easily [16,17]. Namely, we have used hierarchical approximations where only the local part of the measure is renormalized during a RG transformation. Well-known examples are the “approximate recursion formula” [18] or Dyson's hierarchical model (HM) [19,20]. In the following, we only consider the HM with one spin component per site (as in the Ising model). For this model, the existence of a non-trivial unstable fixed point for this model has been proven rigorously [21,22].

In the following, the parameter playing the role of the dimensionality (see section II) will

be tuned in such way that a Gaussian massless fields scales exactly as in three dimensions (see section IIC of Ref. [23] for a more complete discussion of the dimensionality). For this particular choice, the numerical value of this fixed point is known with great precision in a specific system of coordinates [24]. The knowledge of this fixed point together with the demonstrated [25,26,23] effectiveness (in the HT phase) of polynomial approximations for the Fourier transform of the local measure are the key ingredients for an explicit construction of the normal form. In section II, we review the basic facts about the HM and its RG transformation.

A significant effort to prove the existence of normal forms of the RG map of the HM near the unstable (Wilson’s) fixed point was made by Collet and Eckmann [22]. Using the  $\epsilon$ -expansion, it can be stated that for  $\epsilon > 0$  and small enough, a (restricted) normal form can be constructed in a sufficiently small neighborhood of the fixed point. For a precise formulation, the reader is referred to Theorem 4.4 in Ref. [22] and the note related to this theorem.

In the following, we will “follow” the flow all the way down to the HT fixed point. We have chosen value of  $\epsilon$  which is by no mean small but rather corresponding to a value of the dimension between the upper and lower critical values. A more complete construction of the “initial values” of the flows discussed here in terms of the “bare parameters” used in field theoretical perturbative calculations (with flows starting near the Gaussian fixed point) is in progress [27] but will not be discussed here.

#### D. The question of small denominators

In order to complete the program discussed above, we need to consider the question of small denominators near Wilson’s and the HT fixed point. For definiteness, “numerators” and “denominators” are defined as in Eq. (7.23). Our main conclusion is that for very different reasons there seem to be no serious problem at either end.

The question of small denominators near the HT fixed point has been discussed in Ref.

[28]. We give a here short summary. The eigenvalues of the linearized RG map near the HT fixed point are known exactly in the terms of the dimension parameter [22] (see subsection VII B). For the value of the dimension parameter considered here, there exists infinitely many zero denominators. However, in all cases considered in Ref. [28], these zero denominators are “miraculously” compensated by zero numerators. We have found no general explanation for this mechanism. However, it has been checked by numerical methods to all orders relevant for the calculations done here.

On the other hand, near Wilson’s fixed point, our analysis will be mostly one-dimensional and the question is not relevant. We would nevertheless like to mention that there does not seem to be serious problems of small denominators near this fixed point. One can calculate the eigenvalues numerically [23] with great precision using the fixed point of Ref. [24]. We have used these numerical values and made an extensive search [27] for small denominators. The worse case found was that  $\lambda_9$  has four significant digits common with  $\lambda_1^3\lambda_2^2\lambda_{10}$ .

### E. Strategy and main results

Our main strategy has been developed with a simplified model [29] with unidimensional flows. In this article we show that the method can be extended to the multivariable case of the HM. We give a brief sketch of the method, a more precise formulation is given later in sections VI and VII.

We first construct the scaling fields near the HT fixed point  $\tilde{\mathbf{y}}(\mathbf{h})$  in terms of the coordinates  $\mathbf{h}$  in the directions of the eigenvectors of the linearized RG map at the HT fixed point. The boldface notations mean that the quantity is a vector. As shown in [25], finite dimensional approximations give excellent results. If we denote the RG transformation in the  $\mathbf{h}$  coordinates as  $\mathbf{R}(\mathbf{h})$ , and  $\tilde{\lambda}_j$  as the eigenvalue in the  $j$ -th direction, we have by definition of the scaling fields

$$\tilde{y}_j(\mathbf{R}(\mathbf{h})) = \tilde{\lambda}_j \tilde{y}_j(\mathbf{h}). \quad (1.1)$$

For small values of  $\mathbf{h}$ , we have  $\tilde{\mathbf{y}}(\mathbf{h}) \simeq \mathbf{h}$ . One could call the  $\mathbf{h}$ , the “linear scaling fields” or the “real fields” [3] if they have a simple physical interpretation.

Remarkably, there exists simple relations between the initial values of  $\tilde{\mathbf{y}}$  and the infinite volume limit of the derivatives of the free energy with respect to an external magnetic field (connected q-point functions at zero momentum in field theory language). The magnetic susceptibility (second derivative of the free energy) is proportional to the initial value of the first scaling field  $\tilde{y}_1(\mathbf{h}_{in})$ . The fourth derivative of the free energy is proportional to the initial value of the second scaling field. We have checked that a similar relation exists between the sixth (eighth) derivatives and the third (fourth) scaling fields. As explained in subsection VII G, these statements are the consequence of non-trivial cancellations of a certain number of non-linear terms. As for the cancellations of small denominators, we have no general explanation for these remarkable regularities. They substantiate our claim that convergent expansions for the scaling fields with overlapping domains should provide analytical formulas for the thermodynamical quantities. In the following we will mostly discuss the case of the magnetic susceptibility.

The expansion of  $\tilde{y}_1(\mathbf{h}_{in})$  is expected to converge for  $\mathbf{h}_{in}$  small enough, however it might not be very useful near Wilson’s fixed point (and presumably meaningless near the Gaussian fixed point). We then construct the scaling fields near Wilson’s fixed point  $\mathbf{y}(\mathbf{d})$  in terms of the coordinates  $\mathbf{d}$  in the directions of the eigenvectors of the linearized RG map at that fixed point. The  $\mathbf{d}$ ’s can be expressed in terms of the  $\mathbf{h}$ ’s by a shift followed by a linear transformation. With notations similar to Eq. (1.1),

$$y_j(\mathbf{R}(\mathbf{d})) = \lambda_j y_j(\mathbf{d}). \quad (1.2)$$

Given that the leading critical exponent for the susceptibility  $\gamma$  is equal to  $-\ln \tilde{\lambda}_1 / \ln \lambda_1$ , it is clear that  $y_1^\gamma \tilde{y}_1$  is RG-invariant. We can then factor out the susceptibility into a singular part and a RG invariant part:

$$\chi \propto (y_1(\mathbf{d}(\mathbf{h}_{in})))^{-\gamma} [(y_1(\mathbf{d}(\mathbf{h}_{in})))^\gamma \tilde{y}_1(\mathbf{h}_{in})]. \quad (1.3)$$

The expression in bracket is RG-invariant and does not need necessarily to be evaluated for initial values of  $\mathbf{h}$ . We can use the  $n$ -th iterate of these values  $\mathbf{R}^n(\mathbf{h}_{in})$  for any  $n$  and get the same answer for the RG-invariant. In particular, we can choose  $n$  is such a way that the flow is “in between” the two fixed points considered here, in a region where the two expansions have a chance to be valid. The main results presented in this article are numerical evidence that this procedure actually works. In other words, that there exists an overlap between the domains where approximate expansions of the scaling fields scale as they should.

It should be noted that since the RG considered here is discrete (it is constructed by iterating  $\mathbf{R}$  an integer number of times), RG-invariant does not mean independent of  $\mathbf{h}_{in}$ . There is room for log-periodic corrections, which have been first noticed by Wilson [18], discussed in general in Ref. [30] and observed in the HT expansion of the HM in Refs. [16,17]. These corrections are studied for the simplified model in subsection VID. Even though, these corrections are generally small, they can be a nuisance in HT expansions.

It would be interesting to compare the expression (1.3) with the one obtained by Aharony and Fisher in Ref. [31] using the scaling form of the free energy. For this purpose we need to express  $\mathbf{d}$  in terms of the reduced temperature. This requires a detailed analysis of the the initial values of the flows which as explained above, is outside the scope of this investigation. Our expression has room for subleading corrections associated with irrelevant variables and could be compared with Refs. [32,33]. We have checked numerically [34] that some of the predictions of these two papers are correct for the HM. We are confident that a detailed check of the scaling and correction-to-scaling hypotheses is feasible and interesting, however this will not be discussed here.

## F. The content of this article

The article is organized as follows. In section II, we review the basic facts about the HM and its RG transformation. We present a variant of the truncation method proposed in Ref. [25] which will be used in the rest of the article. We also clarify the relationship between

this truncation and the HT expansion.

In the next four sections, we present, explain and illustrate the main ideas with a simplified one-variable model [29] where all the calculations are not too difficult and where the small denominator problem is obviously absent. This model is simply a quadratic map with two fixed points, one stable and one unstable. The one-variable model is presented and motivated in section III, the scaling fields are constructed in section IV and their convergence studied (in terms of the numerical values of the coefficients) in section V. These results will be used as references when a similar analysis is conducted for the HM in the following sections. The susceptibility is calculated in section VI. The most important result for these four sections is illustrated Fig. 12 which shows that the expansion of the scaling fields scale accurately in overlapping regions. In this section, we also resolve the log-periodic corrections up to second order.

The rest of the article is devoted to generalizing the construction for the HM, for which the RG transformation can be approximated by a multivariable quadratic map. In section VII, we show how to choose the coordinates in order to solve the linear problem. In section VIII, we present approximations which allow one to calculate nonlinear expansions for the scaling fields. Finally, the questions of convergence and scaling are discussed in section IX. The most important result is illustrated in Fig. 23 which indicates a proper overlap.

## II. DYSON'S HIERARCHICAL MODEL

In this section, we review the basic facts about the RG transformation of the HM to be used in the rest of the paper. In order to avoid useless repetitions, we will refer the reader to Ref. [22,25] for a more complete discussion. In the following, we will emphasize new material such as the various possibilities available for the truncation procedure and the relationship between the truncation and the HT expansion.

## A. The RG transformation

The energy density (or action in the field theory language) of the HM has two parts. One part is non-local (the “kinetic term”) and invariant under a RG transformation. Its explicit form can be found, for instance, in Ref. [22] or in section II of Ref. [35]. The other part is a sum of local potentials given in terms of a unique function  $V(\phi)$ . The exponential  $e^{-V(\phi)}$  will be called the local measure and denoted  $W_0(\phi)$ . For instance, for Landau-Ginsburg models, the measures are of the form  $W_0(\phi) = e^{-A\phi^2 - B\phi^4}$ , but we can also consider limiting cases such as a Ising measure  $W_0(\phi) = \delta(\phi^2 - 1)$ . Under a block spin transformation which integrates the spin variables in “boxes” with two sites, keeping their sum constant, the local measure transforms according to the integral formula

$$W_{n+1}(\phi) = \frac{C_{n+1}}{2} e^{(\beta/2)(c/4)^{n+1}\phi^2} \int d\phi' W_n\left(\frac{\phi - \phi'}{2}\right) W_n\left(\frac{\phi + \phi'}{2}\right) , \quad (2.1)$$

where  $\beta$  is the inverse temperature (or the coefficient in front of the kinetic term) and  $C_{n+1}$  is a normalization factor to be fixed at our convenience.

We use the Fourier transform

$$W_n(\phi) = \int \frac{dk}{2\pi} e^{ik\phi} \hat{W}_n(k) . \quad (2.2)$$

We introduce a rescaling of  $k$  by a factor  $u/s^n$ , where  $u$  and  $s$  are constants to be fixed at our convenience, by defining

$$R_n(k) \equiv \hat{W}_n\left(\frac{uk}{s^n}\right) , \quad (2.3)$$

In the following, we will use  $s = 2/\sqrt{c}$ . For  $c = 2^{1-2/D}$ , this corresponds to the scaling of a massless gaussian field in  $D$  dimensions. Contrarily to what we have done in the past, we will here absorb the temperature in the measure by setting  $u = \sqrt{\beta}$ . With these choices, the RG transformation reads

$$R_{n+1}(k) = C_{n+1} \exp\left[-\frac{1}{2} \frac{\partial^2}{\partial k^2}\right] \left[R_n\left(\frac{\sqrt{c}k}{2}\right)\right]^2 . \quad (2.4)$$

We fix the normalization constant  $C_n$  so that  $R_n(0) = 1$ . For an Ising measure,  $R_0(k) = \cos(\sqrt{\beta}k)$ , while in general, we have to numerically integrate to determine the coefficients of  $R_0(k)$  expanded in terms of  $k$ .

If we Taylor expand about the origin,

$$R_n(k) = \sum_{l=0}^{\infty} a_{n,l} k^{2l} , \quad (2.5)$$

(where  $a_{n,0} = 1$ ) then the finite-volume susceptibility is

$$\chi_n = -2 \frac{a_{n,1}}{\beta} \left( \frac{2}{c} \right)^n . \quad (2.6)$$

The susceptibility  $\chi$  is defined as

$$\chi \equiv \lim_{n \rightarrow \infty} \chi_n . \quad (2.7)$$

The susceptibility tends to a finite limit for  $0 \leq \beta < \beta_c$ , where  $\beta_c$  is a constant depending on  $c$ . For  $\beta$  equal to or larger than  $\beta_c$ , the definition of  $\chi$  requires a subtraction (see e. g., Ref. [35] for a practical implementation). In the following, we will only consider the HT phase ( $\beta < \beta_c$ ).

We have eliminated  $\beta$  from the mapping, moving it to the initial local measure. The mapping has then fixed points independent of the temperature. One of them is the “universal function”  $U(k)$  found empirically in Ref. [26,23] and which can be written with great accuracy using numerical coefficients provided by Koch and Wittwer in Ref. [24]. The initial measure as a function of  $\beta$  determines a line of initial conditions in the parameter space, running from the HT fixed point, where all the initial parameters are zero, to the critical surface ( $\beta = \beta_c$ ).

We can derive an explicit form for  $a_{n+1,l}$  in terms of  $a_{n,l}$ .

$$a_{n+1,l} = \frac{u_{n,l}}{u_{n,0}} , \quad (2.8)$$

where

$$u_{n,l} \equiv \sum_{i=0}^{\infty} \frac{(-\frac{1}{2})^i (2(l+i))!}{s^{2(l+i)} i! (2l)!} \sum_{p+q=l+i} a_{n,p} a_{n,q} . \quad (2.9)$$

## B. The high-temperature expansion

To study the susceptibility not too far from the HT fixed point, we can expand  $\chi$  in terms of  $\beta$ . Since we choose the scaling factor  $u$  so that  $\beta$  is eliminated from the recursion, we find that  $a_{0,l} \propto \beta^l$ . From the form of the recursion, Eq. (2.9), we can see that  $a_{n,l}$  will always have  $\beta^l$  as the leading power in its HT expansion (since  $p+q \geq l$ ). If we want  $R(k)$  expanded to order  $\beta^{m_{max}}$ , we will use the truncated recursion formula

$$[u_{n,l}]_{m_{max}} = \sum_{i=0}^{m_{max}-l} \frac{(-\frac{1}{2})^i (2(l+i))!}{(4/c)^{(l+i)} i! (2l)!} \sum_{p+q=l+i} [a_{n,p} a_{n,q}]_{m_{max}} , \quad (2.10)$$

where the notation  $[\dots]_{m_{max}}$  means that the expression in brackets should be expanded up to order  $m_{max}$  in  $\beta$ . We define the coefficients of the expansion of the infinite-volume susceptibility by

$$\chi(\beta) = \sum_{m=0}^{\infty} b_m \beta^m . \quad (2.11)$$

We define  $r_m \equiv b_m/b_{m-1}$ , the ratio of two successive coefficients, and introduce quantities [14], called the extrapolated ratio ( $\hat{R}_m$ ) and the extrapolated slope ( $\hat{S}_m$ ), defined by

$$\hat{R}_m \equiv m r_m - (m-1) r_{m-1} , \quad (2.12)$$

and

$$\hat{S}_m \equiv m S_m - (m-1) S_{m-1} , \quad (2.13)$$

where

$$S_m \equiv \frac{-m(m-1)(r_m - r_{m-1})}{m r_m - (m-1) r_{m-1}} , \quad (2.14)$$

is called the normalized slope. If we use the expansion

$$\chi \simeq (\beta_c - \beta)^{-\gamma} (A_0 + A_1 (\beta_c - \beta)^\Delta + \dots) , \quad (2.15)$$

and assume that  $A_0$  and  $A_1$  are constants, we find

$$\hat{S}_m = \gamma - 1 - Km^{-\Delta} + O(m^{-2}) , \quad (2.16)$$

where  $K$  is a constant. However, if we calculate this quantity for the HM, we find oscillations (see Refs. [16,17]). For comparison with results described later, Fig. 2 shows these oscillations in the extrapolated slope.

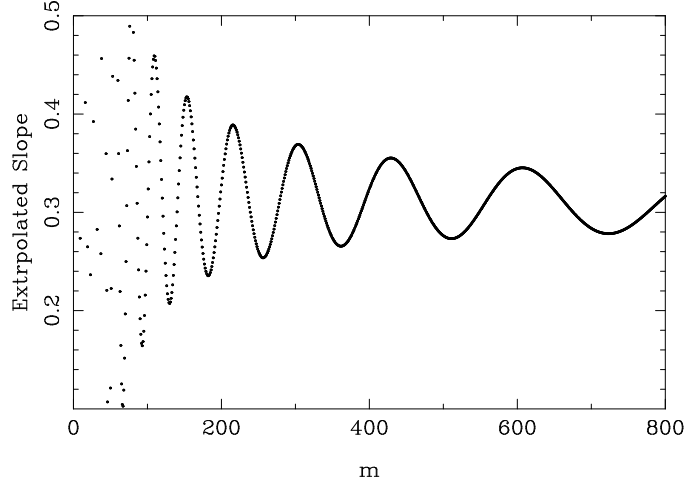


FIG. 2. The extrapolated slope ( $\hat{S}$ ) versus  $m$  for the HM with  $c = 2^{1/3}$ .

### C. The truncation approximation

The HT expansion can be calculated to very high order, however, due to a large number of subleading corrections, this is a very inefficient way to obtain information about the critical behavior. In Ref. [25], it was found that one can obtain much better results by altering Eq. (2.10) . First, we can retain a much smaller number of terms in the sum (originally from 1 to  $m_{max} - l$ ) than in the expansions  $[\dots]_{m_{max}}$ . As an example, one can calculate the 1000-th HT coefficient of  $\chi$  with 16 digits of accuracy using only 35 terms in the sum. Second, we can simply replace the expansions  $[\dots]_{m_{max}}$  by numerical values. This is equivalent to consider the polynomial approximation

$$R_n(k) \simeq \sum_{l=0}^{l_{max}} a_{n,l} k^{2l} , \quad (2.17)$$

for some integer  $l_{max}$ . The mapping is then confined to an  $l_{max}$ -dimensional space.

There remains to decide if one should or not truncate to order  $k^{2l_{max}}$  after squaring  $R_n$ . This makes a difference since the exponential of the second derivative has terms with arbitrarily high order derivatives. Numerically, one gets better results at intermediate values of  $l_{max}$  by keeping all the terms in  $R_n^2$ . In addition, for the calculations performed later, the intermediate truncation pads the “structure constants” of the maps (see sec. VII) with about fifty percent of zeroes. A closer look at section VII, may convince the reader that not truncating after squaring is more natural because we obtain correct (in the sense that they keep their value when  $l_{max}$  is increased) structure constants in place of these zeroes. We have thus followed the second possibility where we truncate only once at the end of the calculation. With this choice

$$u_{n,l} \simeq \sum_{i=0}^{2l_{max}-l} \frac{(-\frac{1}{2})^i (2(l+i))!}{(4/c)^{(l+i)} i! (2l)!} \sum_{p+q=l+i} a_{n,p} a_{n,q} . \quad (2.18)$$

Compared to the HT expansion, the initial truncation to order  $l_{max}$  is accurate up to order  $\beta^{l_{max}}$ . After one iteration, we will miss terms of order  $\beta^{l_{max}+1}$  but we will also generate some of the contributions of order  $\beta^{2l_{max}}$  (but not all of them). After  $n$  iterations we generate some of the terms of order  $\beta^{2^n l_{max}}$  as in superconvergent expansions.

### III. A ONE-VARIABLE MODEL

Before attacking the multivariable expansions of the scaling fields, we would like to illustrate the main ideas and study the convergence of series with a simple one variable example which retains the important features: a critical temperature, RG flows going from an unstable fixed point to a stable one, and log-periodic oscillations in the susceptibility.

In order to obtain a simple one-variable model, we first consider the  $l_{max} = 1$  truncation using Eq. (2.18). The mapping is then reduced to only one variable. The mapping takes the form:

$$a_{n+1,1} = \frac{(c/2)a_{n,1} - (3c^2/8)a_{n,1}^2}{1 - (c/2)a_{n,1} + (3c^2/16)a_{n,1}^2} , \quad (3.1)$$

Expanding the denominator and keeping terms in the mapping only up to order 2 in  $a_{n+1,1}$ , we obtain

$$a_{n+1,1} = (c/2)a_{n,1} - (c^2/8)a_{n,1}^2. \quad (3.2)$$

From Eq. (2.6), we can put this recursion directly in terms of the (truncation approximated) susceptibility:

$$\chi_{n+1} = \chi_n + \frac{\beta}{4} \left(\frac{c}{2}\right)^{n+1} \chi_n^2. \quad (3.3)$$

This approximate equation was successfully used in Ref. [25] to model the finite-size effects. If we expand  $\chi$  (the limit of  $\chi_n$  when  $n$  becomes infinite) in  $\beta$ , and define the extrapolated slope,  $\hat{S}_m$ , as in Eq. (2.13), we see oscillations in Fig. 3 quite similar to those in the HM. (Fig. 2).

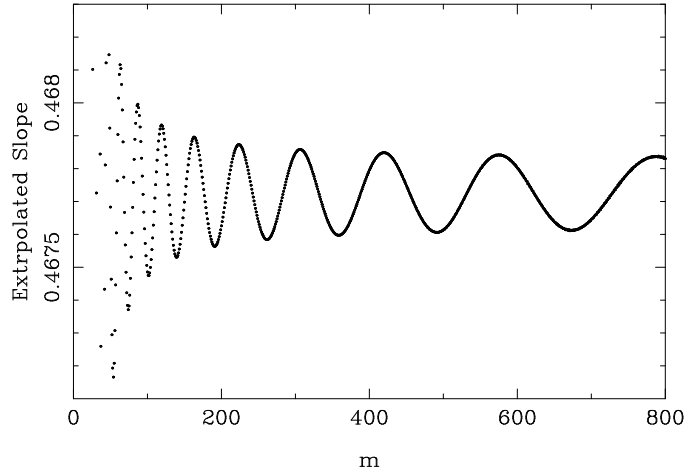


FIG. 3. The extrapolated slope ( $\hat{S}_m$ ) versus  $m$  for the HT of  $\chi$  calculated from the simplified recursion Eq. (3.3) with  $c = 2^{1/3}$ .

In the following, we use the notation  $\xi \equiv c/2$  and we only consider the case  $\chi_0 = 1$  as in the Ising model. Our analysis will be simplified if we remove the explicit  $n$ -dependence of the recursion. For this purpose, we define a new quantity,  $h_n$ , such that

$$\chi_n \equiv \frac{\alpha h_n}{\xi^n}, \quad (3.4)$$

where  $\alpha$  is an arbitrary constant. This gives the recursion

$$h_{n+1} = \xi h_n + \frac{\beta}{4} \xi^2 \alpha h_n^2 . \quad (3.5)$$

The fixed points of this map are

$$h^* = 0, \frac{4(1-\xi)}{\alpha\beta\xi^2} . \quad (3.6)$$

We can choose  $\alpha$  so that the non-zero fixed point is equal to one:

$$\alpha = \frac{4(1-\xi)}{\beta\xi^2} . \quad (3.7)$$

This has the nice effect of making the fixed points independent of  $\xi$  and  $\beta$ . Also,  $\beta$  is removed entirely from the map, making it only dependent on  $\xi$ :

$$h_{n+1} = \xi h_n + (1-\xi)h_n^2 . \quad (3.8)$$

We call this map the “ $h$ -map”. We recover the susceptibility from:

$$\chi_n = \frac{4(1-\xi)}{\beta\xi^2} \frac{h_n}{\xi^n} . \quad (3.9)$$

Recalling that  $\chi_0 = 1$ , we have

$$h_0 = \frac{\beta\xi^2}{4(1-\xi)} , \quad (3.10)$$

allowing us to write

$$\chi_n = \frac{h_n}{h_0} \xi^{-n} \quad (3.11)$$

for non-zero  $h_0$  ( $h_0 = 0$  means that  $\beta = 0$  and  $\chi_n = 1$  for all  $n$ ).

If we iterate the recursion Eq. (3.8), we find that for  $0 \leq h_0 < 1$ ,  $h_n \rightarrow 0$  as  $n \rightarrow \infty$ . Correspondingly, for  $n \rightarrow \infty$ ,  $\chi_n$  approaches a constant,  $\chi$ , as we saw by using the original recursion. For  $h_0 = 1$ ,  $h_n = 1$  for all  $n$ . For  $h_0 > 1$ ,  $h_n \rightarrow \infty$  for  $n \rightarrow \infty$ . This is the same behavior of the susceptibility expected as the temperature ( $\beta$ ) crosses the critical value. The adjustable parameter in  $h_0$  is  $\beta$ , so we see that  $h_0 = 1$  corresponds to  $\beta = \beta_c$ , consequently

$$\beta_c = \frac{4(1-\xi)}{\xi^2} . \quad (3.12)$$

In Fig . 4, we show the values of  $h_n$  for different values of  $h_0$ . This figure indicates that the shape of the function is independent of  $h_0$ .

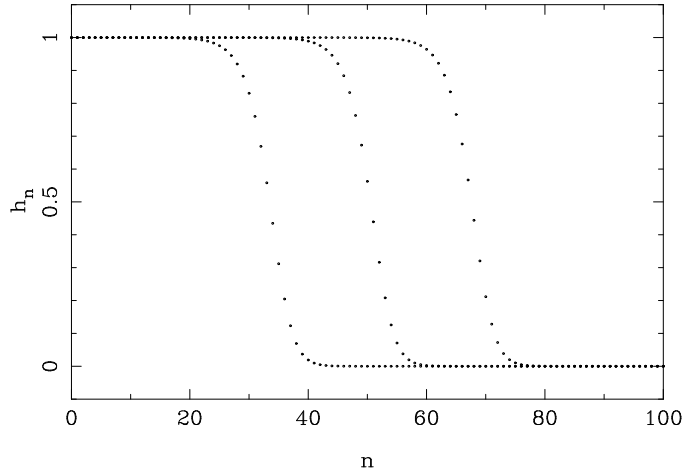


FIG. 4.  $h_n$  versus  $n$  for  $\xi = 0.5$ . Here  $h_0 = 1 - 10^{-6}$ ,  $1 - 10^{-9}$ , and  $1 - 10^{-12}$ .

To understand the behavior of the  $h$ -map, we need to investigate the stability of the fixed points. We find:

$$\left( \frac{dh_{n+1}}{dh_n} \right)_{h_n=0} = \xi , \quad (3.13)$$

and

$$\left( \frac{dh_{n+1}}{dh_n} \right)_{h_n=1} = 2 - \xi . \quad (3.14)$$

In the following, we only consider  $0 < \xi < 1$ , so the zero fixed point is stable, while the other is unstable. All the  $h_0$  between zero and the unstable fixed point are attracted toward the stable fixed point. Also note that for all  $h_0$  greater than the unstable fixed point,  $h_n \rightarrow \infty$ . For  $h_0$  at the unstable fixed point,  $h_n = 1$  for all  $n$ . So then  $\chi_n = \xi^{-n}$ . This diverges, since  $\xi < 1$ .

Note that the  $h$ -map can be put in Ref. [36],

$$x_{n+1} = 1 - \mu x_n^2 , \quad (3.15)$$

with

$$\mu = (\xi/4)(\xi - 2) , \quad (3.16)$$

by using a linear transformation. With their parametrization, the first bifurcation where the fixed point becomes unstable and a cycle 2 develops occurs at  $\mu = 0.75$ . This corresponds

to  $\xi=3$  or  $-1$  which is outside of the region where we will study the map in the following (clearly, a cyclic behavior means no thermodynamic limit).

We can expand the map about the unstable fixed point,  $h_n = 1$ .

$$h_{n+1} = 1 + (2 - \xi)(h_n - 1) + (1 - \xi)(h_n - 1)^2. \quad (3.17)$$

We denote the eigenvalue near the critical point by  $\lambda$  and we have  $\lambda \equiv 2 - \xi$ . If we define

$$d_n \equiv 1 - h_n, \quad (3.18)$$

then:

$$d_{n+1} = \lambda d_n + (1 - \lambda) d_n^2, \quad (3.19)$$

with the starting value  $d_0 = 1 - \beta/\beta_c$ . We call this map the “ $d$ -map”.

Note the similarity of the  $d$ -map to the original  $h$ -map. We can introduce a duality transformation [29] between the two maps which interchanges  $h_n \leftrightarrow d_n$  and  $\xi \leftrightarrow \lambda$ . If the duality transformation is applied twice, we return to the original quantities. For  $0 < h_0 < 1$ , we also have  $0 < d_0 < 1$  with small values (approaching 0 from above) in one variable corresponding to large values (approaching 1 from below) values in the dual variable.

We would like to construct the susceptibility,  $\chi$ , as a function of  $d_0$ . As a first approximation, we use Eq. (3.19) to linearize near the unstable fixed point ( $d_0 = 0$ ), finding the critical exponent  $\gamma$  in the process. Beginning with a value of  $d_0$  very small ( $\beta$  close to  $\beta_c$ ), then for a certain number of iterations  $d_{n+1} \simeq \lambda d_n$ , so that  $d_n \simeq \lambda^n d_0$ . So as long as  $\lambda^n(1 - \beta/\beta_c) \ll 1$ , then  $h_n \simeq 1$  and  $\chi_n \simeq \xi^{-n}$ . If we assume that  $h_n$  stays near 1 for some number of iterations, and then drops quickly, near some  $n = n^*$ , to the region where  $h_n \propto \xi^{-n}$  (thus stabilizing  $\chi$ ), then  $\chi \sim \xi^{-n^*}$ .

Defining  $n^*$  by  $\lambda^{n^*} d_0 = 1$ , we have

$$n^* = -\frac{\ln d_0}{\ln \lambda}, \quad (3.20)$$

which gives

$$\chi \sim \xi^{-n^*} = \left(1 - \frac{\beta}{\beta_c}\right)^{\frac{\ln \xi}{\ln \lambda}}. \quad (3.21)$$

Using the usual notation for the critical exponent, the leading singularity is given by  $(1 - \beta/\beta_c)^{-\gamma}$ . So we have

$$\gamma = \frac{\ln(1/\xi)}{\ln \lambda}, \quad (3.22)$$

or, equivalently:

$$\lambda^\gamma = \frac{1}{\xi}. \quad (3.23)$$

We can divide the leading singularity out of  $\chi$  and plot the remainder near to the critical point (Fig. 5).

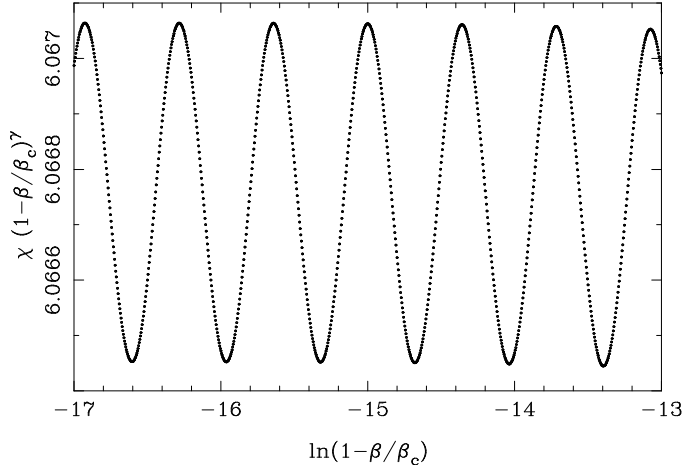


FIG. 5. Oscillations near the critical point. The susceptibility is generated from the recursion Eq. (3.19) with  $\lambda = 1.9$ , while  $\gamma$  and  $\beta_c$  are calculated from the formulas derived in the text.

We see periodic oscillations with respect to the variable  $\ln(1 - \frac{\beta}{\beta_c})$  which have period of  $\ln \lambda$ . The linear approximation gives no clue as to the origins of the oscillations. To understand this, as well as the higher-order corrections to the leading singularity, we need to expand  $d_n$  to higher order in  $d_0$ .

#### IV. SCALING FIELDS IN THE ONE-VARIABLE MODEL

In this section, we show that the idea of scaling field comes naturally as a way to express the susceptibility of the one-variable model in terms of  $d_0$ .

### A. $d_n$ as a function of $d_0$

We can find  $d_n$  in terms of  $d_0$  by expanding

$$d_n = \sum_{l=1}^{\infty} q_{n,l} d_0^l . \quad (4.1)$$

and plugging into Eq. (3.19). We find

$$q_{n,l} = \lambda q_{n-1,l} + (1 - \lambda) \sum_{j=1}^{l-1} q_{n-1,j} q_{n-1,l-j} . \quad (4.2)$$

Given the initial coefficients, i.e.  $q_{1,1} = \lambda$ ,  $q_{1,2} = (1 - \lambda)$ , and  $q_{1,j} = 0$  for  $j > 2$ , we can find all the coefficients at any  $n$ . For example,

$$q_{n,2} = \frac{\lambda^n (1 - \lambda^n)}{\lambda} . \quad (4.3)$$

Finding forms for the coefficients explicitly in terms of  $\lambda$  and  $n$  by this direct method quickly becomes difficult. We will show that this task can be simplified by introducing the scaling fields.

As noticed before, the transition region from  $d_n \simeq 0$  to  $d_n \simeq 1$  has a shape which looks independent of  $d_0$  (see Fig. 4 and use Eq. (3.18)). The shape seem to depend only on the value of  $\lambda$ . We can prove this in a restricted way by imagining a new initial value of “ $d_0$ ” which is identical to the current  $d_1$ . The shape of the curve to the right would then be identical to the current case. Likewise, we can reverse the map, getting new values for “ $d_0$ ” which nonetheless generate all the values in the current series  $d_0, d_1, \dots$ . This inverse map is unique, assuming we confine it to only positive values for  $d_n$ , and has the form

$$d_n = \frac{\sqrt{\lambda^2 + 4(1 - \lambda)d_{n+1}} - \lambda}{2(1 - \lambda)} . \quad (4.4)$$

In this case, the renormalization group is a group in the strict sense, since we have defined a unique inverse.

What we would like then is a way of parameterizing  $d_n$  in terms of a function independent of  $n$ . Regardless of our actual  $d_0$ , we can extrapolate backwards, as suggested above, to

another “ $d_0$ ”, which is small enough so that the linearized method works, where each new “ $d_n$ ” scales approximately as  $\lambda^n$  times the “ $d_0$ ”. This suggests using a new parameter, which we call  $y_n$ , that scales exactly like this, so that if  $d_n$  corresponds to  $y_n$ , then  $d_{n+1}$  corresponds to  $y_{n+1} = \lambda y_n$ . This is our first covariant quantity, so-called since it scales exactly the same, regardless of the value of  $n$ .

Let us define a function  $d$  such that  $d(y_n) \equiv d_n$ . From the explicit form of the recursion formula Eq. (2.4) this requirement implies

$$d(\lambda y_n) = \lambda d(y_n) + (1 - \lambda)d^2(y_n) . \quad (4.5)$$

If we let

$$d(y_n) = \sum_{l=1}^{\infty} s_l y_n^l , \quad (4.6)$$

we find that

$$s_l = \frac{1 - \lambda}{\lambda^l - \lambda} \sum_{j=1}^{l-1} s_j s_{l-j} . \quad (4.7)$$

The first coefficient is undetermined. We let  $s_1 \equiv 1$ , so that for small  $y_n$ , we have  $d_n \simeq y_n$ .

The first few coefficients give

$$d(y_n) = y_n - \frac{1}{\lambda} y_n^2 + \frac{2}{\lambda^2(\lambda + 1)} y_n^3 + \dots \quad (4.8)$$

In Fig. 6, we plot  $d(y_n)$  for several values of  $\lambda$ .

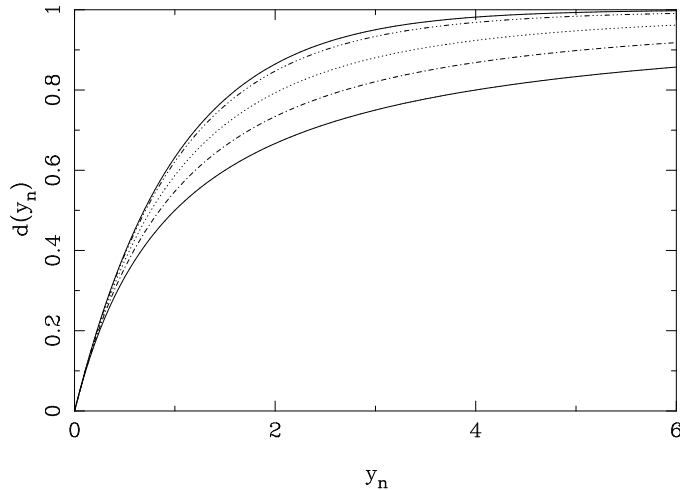


FIG. 6.  $d(y_n)$  for various values of  $\lambda$ . The top and bottom curves represent the  $\lambda \rightarrow 2$  and  $\lambda \rightarrow 1$  limits, respectively. The dash-dot-dot line is  $\lambda = 1.9$ , the dotted line is  $\lambda = 1.6$ , and the dash-dot line is  $\lambda = 1.3$ .

In the limit where  $\lambda \rightarrow 2$ , we can calculate explicitly  $d(y_n)$ . This corresponds to  $\xi = 0$ , so that  $h_{n+1} = h_n^2$ . This is satisfied if  $h_n = e^{ay_n}$ , where  $a$  is arbitrary. So we have  $d_n = 1 - e^{ay_n}$ . The arbitrary value  $a$  can be fixed by requiring  $y_n \simeq d_n$  for small  $d_n$ . This implies  $a = -1$ .

The expression of  $d_n$  as  $d(\lambda^n y_0)$  allows us to interpolate between integral values of  $n$ . In Fig. 7, we show the curve for  $d(y_n)$  superimposed on points generated from the  $d$ -map for  $\lambda = 1.5$ .

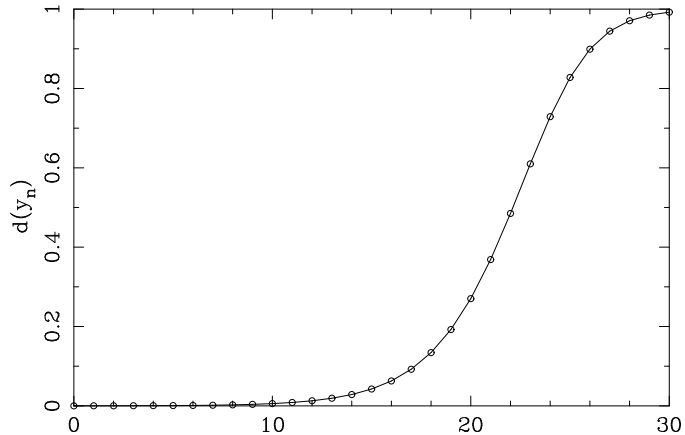


FIG. 7.  $d(y_n)$  plotted against  $n$ . The data points (circles) are generated directly from the  $d$ -map recursion with  $\lambda = 1.5$  and  $d_0 = 10^{-4}$ .

We can invert the series for  $d(y_n)$  in terms of  $y_n$ , defining a new function  $y$ , so that  $y(d_n) = y_n$ . Since we know the coefficients of the  $d(y_n)$  series, we can invert to get  $y$  in terms of  $d_n$ . More directly, we can use  $y_{n+1} = \lambda y_n$ , or

$$y(\lambda d_n + (1 - \lambda)d_n^2) = \lambda y(d_n) , \quad (4.9)$$

along with the constraint  $y(d_n) \simeq d_n$  for small values of  $d_n$ , to construct a series solution. If we let

$$y(d_n) = \sum_{l=1}^{\infty} t_l d_n^l , \quad (4.10)$$

we find that

$$t_l = \frac{-1}{\lambda^l - \lambda} \sum_{j=1}^{\text{int}(l/2)} \frac{(l-j)!}{j!(l-2j)!} \lambda^{l-2j} (1-\lambda)^j t_{l-j} , \quad (4.11)$$

with  $t_l \equiv 1$ . The notation  $\text{int}(l/2)$  means to use the integer part of  $l/2$ . The first few terms give:

$$y(d_n) = d_n + \frac{1}{\lambda} d_n^2 + \frac{2}{\lambda(\lambda+1)} d_n^3 + \dots \quad (4.12)$$

Taking our  $\lambda \rightarrow 2$  example, we can immediately invert our result for  $d(y_n)$ , to find  $y(d_n) = -\ln(1 - d_n)$ .

Having at hand the  $y$ -function and its inverse, we can now as announced reconstruct  $d_n$  in terms of  $d_0$ :

$$d_n = y^{-1}(\lambda^n y(d_0)) . \quad (4.13)$$

### B. $h_n$ as a function of $h_0$

Because of the duality between our two maps, we can easily reproduce all of the above results of the  $d$ -map for the  $h$ -map. Just as with  $d_n$ , we can parameterize  $h_n$  in terms of a covariant variable,  $\tilde{y}_n$ , dual to  $y_n$ . Similarly to before, we define  $h(\tilde{y}_n) \equiv h_n$ , with  $\tilde{y}_n = \xi^n \tilde{y}_0$ . We can also define the inverse function for  $h$ ,  $\tilde{y}$ , where

$$\tilde{y}(\xi h_n + (1 - \xi) h_n^2) = \xi \tilde{y}(h_n) . \quad (4.14)$$

We can immediately carry over all of the results we found for  $d(y_n)$  and  $y(d_n)$  to  $h(\tilde{y}_n)$  and  $\tilde{y}(h_n)$ , replacing  $\lambda$  with  $\xi$ . The new covariant variable behaves similarly to  $y_n$ . However, since  $\xi < 1$ , we see that as  $n \rightarrow \infty$ ,  $\tilde{y}_n \rightarrow 0$ , while as  $n \rightarrow -\infty$ ,  $\tilde{y}_n \rightarrow \infty$ .

## V. LARGE ORDER BEHAVIOR FOR THE ONE-VARIABLE MODEL

In this section we give empirical results concerning the large order behavior of  $y(d)$ ,  $\tilde{y}(h)$  and their inverses. From this, we infer the domain of convergence of the expansions. We

would like to know if the series converge for the ranges of interest. The allowed ranges are 0 to infinity for  $y_n$  and  $\tilde{y}_n$ , and 0 to 1 for  $d_n$  and  $h_n$ .

### A. $d(y)$

For the  $d$ -map, we first examine the extreme allowed values for  $\lambda$ , 1 and 2. For  $\lambda = 2$  ( $\xi = 0$ ), we already found that  $d(y) = 1 - e^{-y}$ . Eq. (4.7) converges in the whole complex plane. At the other end of our range, for  $\lambda \rightarrow 1$  ( $\xi \rightarrow 1$ ), Eq. (4.7) becomes

$$s_l = \frac{-1}{l-1} \sum_{j=1}^{l-1} s_j s_{l-j}, \quad (5.1)$$

so that

$$d(y) = y - y^2 + y^3 - y^4 + \dots \quad (5.2)$$

This converges only for  $0 < y < 1$ , to  $d(y) = y/(1+y)$ .

We use the ratio test to determine convergence for our series. The series will converge in the entire complex plane if  $|s_{l-1}/s_l|$  increases without bound as  $l \rightarrow \infty$ . For all tested values of  $1 < \lambda < 2$ , we found that we could fit a straight line to plots of  $\ln|s_{l-1}/s_l|$  versus  $\ln(l)$  for large enough  $l$  (Fig. 8).

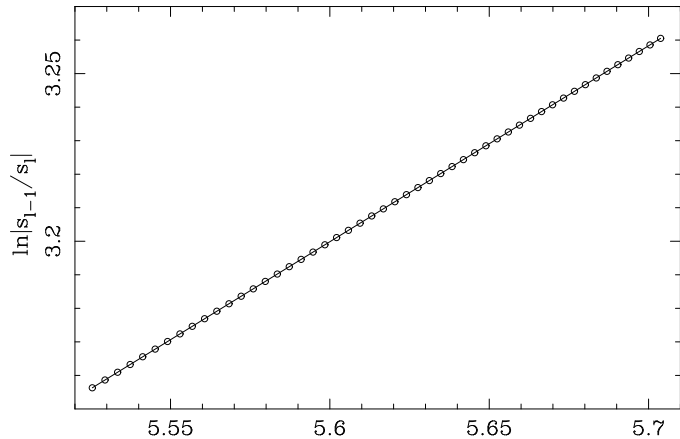


FIG. 8. Linear fit to a logarithmic plot of the ratio of coefficients against the order of the bottom coefficient. Here,  $\lambda = 1.5$ . The slope of the line is 0.584.

Thus for large  $l$ , the coefficients obey the approximate rule

$$\left| \frac{s_l}{s_{l+1}} \right| \simeq Cl^k , \quad (5.3)$$

where we find that  $C$  is always of order 1 (in fact,  $0.9 < C < 1$ ) and  $0 < k < 1$ . Using iteratively this formula, we find that the coefficients decrease like  $C^{-l}(l!)^{-k}$  and consequently the  $d(y)$  should be an entire function. The value of  $k$  can be determined by a linear fit. It seems clear that with  $1 < \lambda < 2$ , the series for  $d(y)$  converges for all  $0 < y < \infty$ . In agreement with the above exact series, for  $\lambda \rightarrow 1$ ,  $C \rightarrow 1$  and  $k \rightarrow 0$ , while for  $\lambda \rightarrow 2$ ,  $C \rightarrow 1$  and  $k \rightarrow 1$ . The intermediate values are given in Fig. 9.

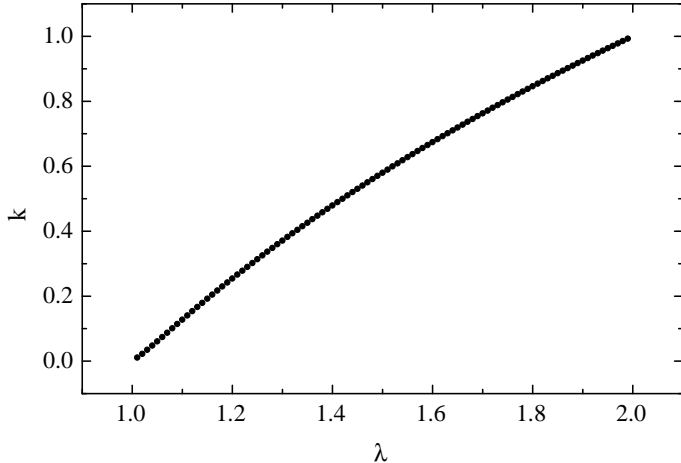


FIG. 9. The exponent  $k$  defined in Eq. (5.3) as a function of  $\lambda$ .

Eq. 5.3 gives us an idea of the number of coefficients we will need to approximate  $d(y)$  for a given value of  $y$ . Assuming that a particular term in the series becomes significant when it is the same size as the previous term, we find that the order that we need in order to get a good approximation goes like

$$l \sim (y/C)^{1/k} . \quad (5.4)$$

### B. $h(\tilde{y})$

We now turn to the dual function,  $h$ . Above, we found the series in  $d(y)$  for  $\lambda \rightarrow 1$ . From this, we can immediately write down  $h(\tilde{y})$  when  $\xi \rightarrow 1$ . The series is identical in form, with  $\lambda$  replaced by  $\xi$ , so that  $h(\tilde{y}) = \tilde{y}/(1 + \tilde{y})$  with an expansion which converges for  $|\tilde{y}| < 1$ . For the general case, we again examine the ratios of successive coefficients,  $|s_l/s_{l+1}|$ . We find the ratios flatten to constant values, for large enough  $l$ , indicating finite radii of convergence. The radii get smaller and vanish as  $\xi$  approaches zero as shown in Fig. 10.

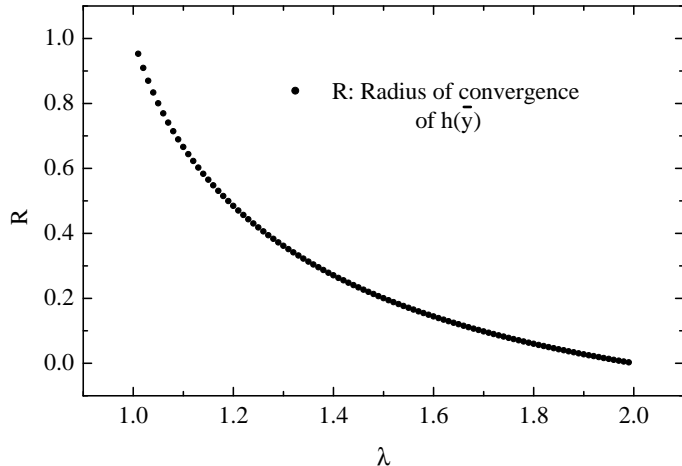


FIG. 10. Radius of convergence of  $h(\tilde{y})$  as a function of  $\lambda = 2 - \xi$ .

Note that for any value of  $\xi$  tried, we found good evidence that  $\lim_{n \rightarrow \infty} \hat{S}_n = -1.5$ , indicating a  $(\tilde{y} - \tilde{y}_c)^{1/2}$  behavior. This is consistent with the existence of a quadratic minimum for the inverse function discussed below.

### C. $y(d)$

We already found above that for  $\lambda = 2$ ,  $y(d) = -\ln(1 - d)$ . This series converges for  $0 < d < 1$ , which is the required range. As  $d \rightarrow 1$ , we reach the HT fixed point and it is not surprising that our series breaks down in this limit. For  $\lambda \rightarrow 1$ , we have, inverting the

$d$ -function found above, that  $y(d) = d/(1-d)$  which also converges for  $0 < d < 1$ . We find empirically from the analysis of ratios that for all  $1 < \lambda < 2$ ,  $y(d)$  converges in the region  $0 < d < 1$ . The analysis of the extrapolated slope for various  $\lambda$  gives convincing evidence that the main singularity has the form

$$y(d) \sim (1-d)^{-1/\gamma} . \quad (5.5)$$

This can be seen with short series when  $\lambda$  is close to one and requires larger and larger series as  $\lambda$  gets close to 2. Illustration of these properties for a particular value of  $\lambda$  are shown in Figs. 16 and 17 where the estimators are compared with those of the HM.

#### D. $\tilde{y}(h)$ )

The  $\tilde{y}(h)$  series behaves similarly to the  $y(d)$ , having a radius of convergence of 1 for all  $\xi$ . In this case, the ratio of coefficients  $t_l/t_{l+1}$  approaches 1 smoothly from below as  $l$  increases, for larger  $\xi$ . Around  $\xi = 0.4$ , small oscillations begin to appear in the curve. As  $\xi$  becomes smaller, these oscillations grow and become quite large for  $\xi$  smaller than 0.1 (Fig. 11). However, in all cases studied, the ratio eventually approaches 1, for large enough  $l$ .

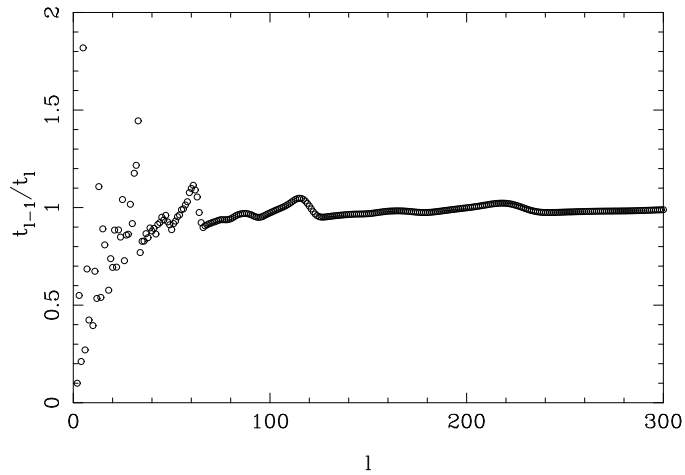


FIG. 11. Ratios of coefficients for  $\tilde{y}(h_n)$  with  $\xi = 0.1$ .

A detailed study shows that if we continue  $\tilde{y}(h)$  for negative values of  $h$  using the series

expansion, the function develops a quadratic minimum when  $h \rightarrow -1$ . The absolute value  $h(-1)$ , in all examples studied, is compatible with the radius of convergence of the inverse function and the square root singularity of the  $h(\tilde{y})$  discussed above.

As one may suspect by looking at Fig. 3, the analysis of the extrapolated slope is intricated. However, if we calculate enough terms and if  $\lambda$  is not too close to 2, we get approximate results which are consistent with a main singularity of the form

$$\tilde{y}(h) \sim (1 - h)^{-\gamma} . \quad (5.6)$$

For instance, just by looking at the asymptotic behavior of Fig. 3, one can see that  $\gamma \simeq 1.4677$ , as expected, with errors of the order  $10^{-4}$ . It is interesting to note the duality [29] between Eqs. (5.5) and (5.6).

## VI. THE SUSCEPTIBILITY OF THE ONE-VARIABLE MODEL

Now that we can calculate  $h_n$  and  $d_n$ , we can construct the infinite volume susceptibility. If we focus on the HT fixed point and the  $h$ -map, we get the HT expansion in terms of  $h_0 = \beta/\beta_c$ . On the other hand, to understand the susceptibility's behavior near the unstable fixed point, we need to expand in terms of  $d_0 = 1 - \beta/\beta_c$ . Finally, we consider the possibility of combining the two expansions in the crossover region.

### A. The HT expansion of the susceptibility

We could find the HT expansion from the finite-volume susceptibility found in the previous section, by taking the large- $n$  limit. Since  $0 < \xi < 1$ , all of the  $\xi^n$  terms will drop out. However, we can also construct the large- $n$  limit directly. Recalling that  $\chi_n = (h_n/h_0)\xi^{-n}$ , and using  $\tilde{y}_n = \xi^n \tilde{y}_0$ , we find that

$$\chi_n = \frac{h_n \tilde{y}_0}{h_0 \tilde{y}_n} = \frac{h(\tilde{y}_n) \tilde{y}_0}{h_0 \tilde{y}_n} . \quad (6.1)$$

The infinite-volume limit becomes:

$$\chi \equiv \lim_{n \rightarrow \infty} \chi_n = \frac{\tilde{y}_0}{h_0} \lim_{n \rightarrow \infty} \frac{h(\tilde{y}_n)}{\tilde{y}_n} . \quad (6.2)$$

Using the  $\tilde{y}$ -expansion for  $h$ , we find

$$\frac{h(\tilde{y}_n)}{\tilde{y}_n} = 1 - \frac{\tilde{y}_n}{\xi} + \dots \quad (6.3)$$

As  $n \rightarrow \infty$ ,  $\tilde{y}_n \rightarrow 0$ , so the infinite volume limit of the susceptibility is:

$$\chi = \frac{\tilde{y}_0}{h_0} = \frac{\tilde{y}(h_0)}{h_0} . \quad (6.4)$$

Using the  $h$ -expansion for  $\tilde{y}$ , we get the HT expansion for the susceptibility:

$$\chi = 1 + \frac{1}{\xi} h_0 + \frac{2}{\xi(1+\xi)} h_0^2 + \dots \quad (6.5)$$

Using  $\chi_n = (h_n/h_0)\xi^{-n}$ , we find the HT expansion for the finite-volume susceptibility (recall that  $h_0 = \beta/\beta_c$ ):

$$\chi_n = 1 + \frac{1 - \xi^n}{\xi} h_0 + \dots \quad (6.6)$$

We can find the error in the finite-volume susceptibility as an approximation to  $\chi$ . For large  $n$  (small  $\tilde{y}_n$ ), we get  $\chi_n \simeq \chi(1 - \tilde{y}_n/\xi) = \chi(1 - \xi^{n-1}\tilde{y}_0)$ . The relative error is then:

$$\frac{\chi - \chi_n}{\chi} \simeq \xi^{n-1}\tilde{y}_0 = \xi^{n-1}h_0\chi . \quad (6.7)$$

This behavior is observed [25] in the approach to infinite volume for the HM. More generally, we see that the scaling fields also contain information about finite-scale effects.

## B. Expansion near the critical point

In addition of using the HT expansion (expressing  $\chi$  in terms of  $h_0$ ), we would also like to have an expansion in terms of the dual variable  $d_0$ . Multiplying the numerator and the denominator of Eq. (6.4) by  $y_0^\gamma$ , we obtain

$$\chi = \frac{\Theta}{(1 - d_0)y(d_0)^\gamma} . \quad (6.8)$$

with

$$\Theta \equiv \tilde{y}_0 y_0^\gamma . \quad (6.9)$$

But since  $\lambda^\gamma = \xi^{-1}$ , we have also

$$\Theta = \tilde{y}_n y_n^\gamma , \quad (6.10)$$

for any  $n$ . In other words,  $\Theta$  is RG invariant. Due to the discrete nature of our RG transformation,  $\Theta$  is not exactly a constant. If expressed in terms of  $\ln(y_0)$ ,  $\Theta$  is a periodic function of period  $\ln\lambda$ . However, for  $\lambda$  not too close to 2, the non-zero Fourier modes are very small (see subsection VID). Note also that the apparent singularity when  $d_0 \rightarrow 1$  is exactly canceled by  $y(d_0)^\gamma$  by virtue of Eq. (5.5).

### C. Numerical evidence for overlapping domains of convergence

As we have seen above,  $\tilde{y}_n y_n^\gamma$  is independent of  $n$ . We can thus pick  $n$  such that we are just in the crossover region and *both* expansions have a reasonable chance to be accurate. In order to test the accuracy of the approximations  $y_{app}(d)$  (series expansion up to a certain order) for various  $n$ , we have prepared an empirical sequences of  $d_n$  starting with  $d_0 = 10^{-8}$ . We have then tested the scaling properties by calculating

$$D_n = | [y_{app}(d_n)/(y_0 \lambda^n)] - 1 | , \quad (6.11)$$

where  $y_0$  was calculated with 16 digits of accuracy by using enough terms in the expansion of  $y(d_0)$ . Optimal approximations are those for which  $D_n \simeq 10^{-16}$ . For such approximation, scaling is as good as it can possibly be given the accuracy of  $y_0$ . Indeed, due to the peculiar way numerical errors propagate [37], one does not reach exactly the expected level  $10^{-16}$  (more about this question in section IX). We can define a similar dual quantity by replacing  $d$  by  $h$  and  $y$  by  $\tilde{y}$ . In this case,  $\tilde{y}_0$  is estimated with the same accuracy as  $y_0$  by stabilizing  $\tilde{y}(h_n)/\xi^n$ , for large enough  $n$ .

We have performed this calculation for  $\lambda = 1.1, 1.5$  and  $1.9$ . The conclusions in the three cases are identical. For  $n$  large enough, the  $D_n$  of  $y$  starts increasing from  $10^{-16}$  until it saturates around 1. By increasing the number of terms in the expansion, we can increase the value of  $n$  for which we start losing accuracy. Similarly, for  $n$  low enough, the  $D_n$  of  $\tilde{y}$  starts increasing etc... We want to know if it is possible to calculate enough terms in each expansion to get scaling with some desired accuracy for both functions. The answer to this question is affirmative according to Fig. 12 for  $\lambda = 1.5$ .

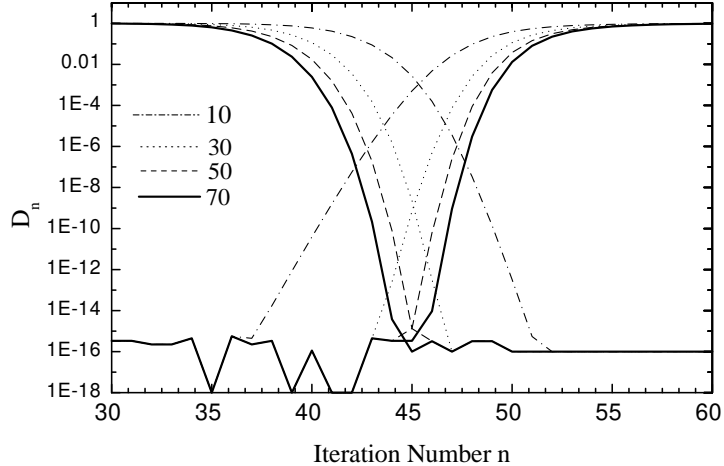


FIG. 12. Departure from scaling  $D_n$  defined in the text, for  $y$  (curves reaching 1 to the right) and  $\tilde{y}$  (curves reaching 1 to the left). In each cases, we have considered approximations of order 10 (dot-dashes), 30 (dots), 50 (dashes) and 70 (solid line). The value of  $\lambda$  is 1.5.

One sees, for instance, that with 10 terms in each series, we have scaling with about 1 part in 1000 near  $n = 45$  for both expansions. The situation can be improved. For 70-70 expansions, an optimal accuracy is reached from  $n = 44$  to 46. For the other values of  $\lambda$  quoted above, similar conclusions are reached, the only difference being the optimal values of  $n$ .

#### D. Analysis of the RG invariant

Another evidence for overlapping convergence is that we can calculate the RG invariant  $\Theta$  for a certain range of  $y_n$ . To evaluate  $\Theta$ , we use the series expansions for  $\tilde{y}$  and  $d$ , cutting each off at some order:

$$\tilde{y}(1 - d(y)) \simeq \sum_{i=1}^{\tilde{m}} t_i \left(1 - \sum_{j=1}^m s_j y^j\right)^i, \quad (6.12)$$

where  $s_l$  and  $t_l$  are the  $l$ th coefficients in the  $d$  and  $\tilde{y}$  series, respectively. The  $d$  series is more accurate the smaller is the value of  $y$ , while the  $\tilde{y}$  series is more accurate for  $d(y)$  close to 1, which means large values of  $y$ . Thus for  $y$  very large, we need many terms in the  $d$  series, while we need less terms in the  $\tilde{y}$  series. On the other hand, when  $y$  is very small, we need a large value for  $\tilde{m}$  and a relatively small  $m$ . We have found that, given a fixed value of  $m + \tilde{m}$ , the most accurate values for  $\Theta$  are obtained when  $m \simeq \tilde{m}$ . In Fig. 13, we show  $\Theta$  calculated by keeping 50 terms each in the expansions for  $y$  and  $\tilde{y}$ . The result is plotted against  $\ln(y_0)$ . We used  $\xi = 0.1$ , which makes the oscillations much larger than, for example, near to  $\xi = 2^{-2/3}$ . Near the fixed points, we need more terms in the appropriate series to get accurate results.

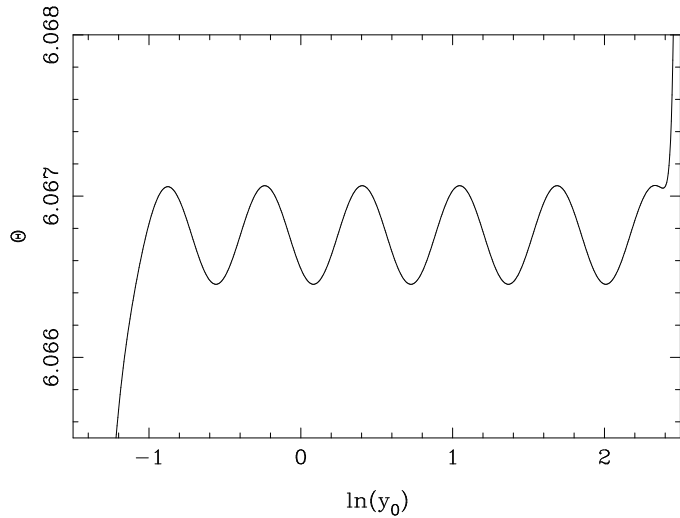


FIG. 13. The invariant function  $\Theta$ , calculated at  $\xi = 0.1$ , and plotted against  $\ln(y_0)$ .

We can study the oscillation we see in  $\Theta$  by looking at its Fourier expansion. Since  $\Theta$  is

periodic in  $\ln y_0$ , we can express

$$\Theta(y_0) = y_0^\gamma \tilde{y}(1 - d(y_0)) = \sum_p a_p e^{ip\omega \ln y_0}, \quad (6.13)$$

where  $\omega \equiv 2\pi/\ln \lambda$ . The coefficients are given as

$$a_p = \frac{1}{\ln \lambda} \int_{y_a}^{\lambda y_a} y^{\gamma-1-ip\omega} \tilde{y}(1 - d(y)) dy, \quad (6.14)$$

for some  $y_a$  of our choice.

As an example, we calculate  $a_0$  for  $\xi = 0.1$  where the oscillations are not too small. The choice of the interval of integration can be inferred from Fig. 13. If we had infinite series, the function would be exactly periodic. For finite series, we see that  $y_a$  cannot be too large or too small. For intermediate values, we obtain  $a_0 \simeq 6.06676$ . In Fig. 14, we show this constant term subtracted from the  $\Theta$  we evaluated above. What remains is oscillations about 0. We also calculated  $a_1$  (using  $y_a = \lambda$  so that we keep information about the phase constant as well as the amplitude). We construct the first oscillating mode from this, and in Fig. (15) we show the result of subtracting out this in addition to the constant term. We are left with even smaller oscillations, from the  $a_2$  term.

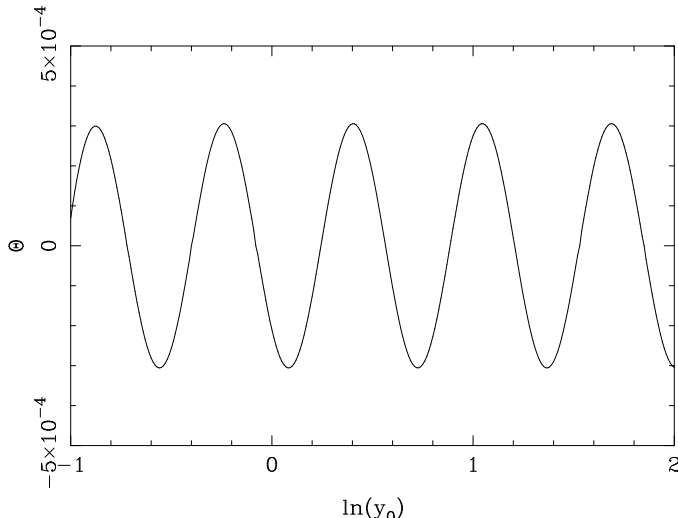


FIG. 14. Same as previous plot, with the constant term from the Fourier expansion subtracted out.

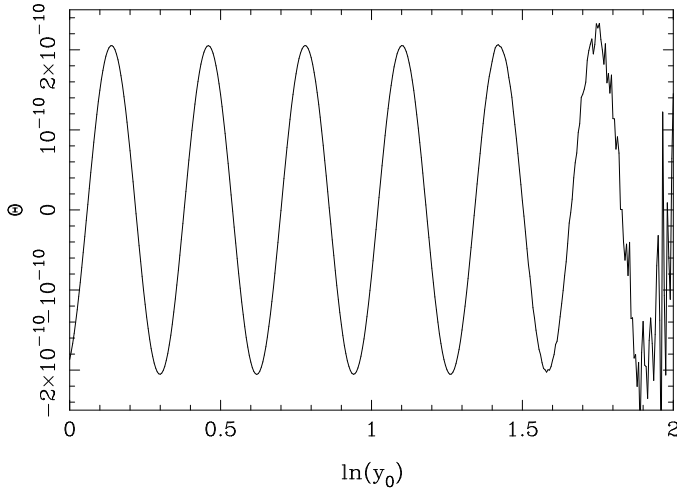


FIG. 15. Same as previous plot, with first oscillating term from the Fourier expansion subtracted out.

In Fig. 15, one notices that when  $\ln(y_0)$  is of the order of 1.7, the breakdown of the approximation starts with small numerical noise before the complete breakdown for larger values occurs (see also Fig. 13).

## VII. SCALING FIELDS IN THE HIERARCHICAL MODEL

In the one-variable model, we learned that we could express the basic mapping coordinates,  $h_n$ , the distance from the HT fixed point, in terms of either of two new variables,  $y_n$  or  $\tilde{y}_n$ . The first of these variables transforms multiplicatively with  $\lambda$ , the eigenvalue near the unstable fixed point, while the second transforms multiplicatively with  $\xi$ , the eigenvalue near the HT fixed point.

We would like to extend these methods to Dyson's HM. We will express the coordinates of the model in terms of two new sets of variables  $y_{n,1}, \dots, y_{n,l_{max}}$  and  $\tilde{y}_{n,1}, \dots, \tilde{y}_{n,l_{max}}$ , where  $l_{max}$  is equal to the number of coordinates we keep in the mapping. These are the scaling fields.

Near to the unstable fixed point we find a set of eigenvectors and eigenvalues which control the RG flows in the linearized region. We use the notation  $\lambda_i$  for the  $i$ th eigenvalue, ordered in size from greatest to least. For each of these eigenvalues, we introduce a variable

$y_{n,i}$  which transforms under the RG transformation as  $y_{n+1,i} = \lambda_i y_{n,i}$ . We denote  $\tilde{\lambda}_i$  for the eigenvalues in the linear HT region, similarly defining variables which transform as  $\tilde{y}_{n+1,i} = \tilde{\lambda}_i \tilde{y}_{n,i}$ . Then we can expand each of the coordinates in terms of each set of scaling fields. Our first task will be to use special coordinates where the problem will be solved at the linear level. To use a relativistic analogy, the transformations leading to such a system of coordinates (the “linear scaling variables”), can be interpreted as a “translation” or shift and a “rotation” or more generally a linear transformation.

### A. Transformation properties under translation

We re-express the basic recursion in terms of a new set of parameters, which give the distance from the nontrivial fixed point. For notational convenience, we first rewrite the unnormalized recursion given in Eq. (2.18), using the “structure constants”:

$$u_{n,\sigma} = \Gamma_{\sigma}^{\mu\nu} a_{n,\mu} a_{n,\nu} , \quad (7.1)$$

with

$$\Gamma_{\sigma}^{\mu\nu} = \begin{cases} (c/4)^{\mu+\nu} \frac{(-1/2)^{\mu+\nu-\sigma} (2(\mu+\nu))!}{(\mu+\nu-\sigma)!(2\sigma)!} & , \quad \text{for } \mu + \nu \geq \sigma \\ 0 & , \quad \text{otherwise} . \end{cases} \quad (7.2)$$

These zeroes can be understood as a “selection rule” associated with the fact that  $a_{n,l}$  is of order  $\beta^l$  as explained in section II. If we follow the truncation procedure explained in section II, the indices simply run over a finite number of values. We use “relativistic” notations. Repeated indices mean summation. The greek indices indices  $\mu$  and  $\nu$  go from 0 to  $l_{max}$ , while latin indices  $i, j$  go from 1 to  $l_{max}$ . Obviously,  $\Gamma_{\sigma}^{\mu\nu}$  is symmetric in  $\mu$  and  $\nu$ . By construction,  $a_{n,0} = 1$  and we can write the normalized recursion in the form:

$$a_{n+1,l} = \frac{\mathcal{M}_l^i a_{n,i} + \Gamma_l^{ij} a_{n,i} a_{n,j}}{1 + \mathcal{M}_0^i a_{n,i} + \Gamma_0^{ij} a_{n,i} a_{n,j}} , \quad (7.3)$$

with

$$\mathcal{M}_{\eta}^i = 2\Gamma_{\eta}^{0i} . \quad (7.4)$$

Let assume that we know a fixed point of the recursion formula  $a_{n,l} = a_l^*$ . We then introduce intermediate variables  $g_{n,l}$  which are zero at the fixed point:

$$a_{n,l} \equiv a_l^* + g_{n,l} . \quad (7.5)$$

Plugging this relation into Eq. (7.3), using the fixed point properties, subtracting the fixed point and reducing to the same denominator, we obtain a recursion formula for the  $g_{n,l}$  having the same form as Eq. (7.3) with the substitutions

$$\Gamma_\eta^{ij} \rightarrow \frac{1}{u_0^*} (\Gamma_\eta^{ij} - (1 - \delta_{\eta 0}) a_\eta^* \Gamma_0^{ij}) , \quad (7.6)$$

and

$$\mathcal{M}_\eta^i \rightarrow \frac{1}{u_0^*} (\mathcal{M}_\eta^i + 2\Gamma_0^{ij} a_j^* + (1 - \delta_{\eta 0}) (\mathcal{M}_0^i + 2\Gamma_0^{ij} a_j^*) a_\eta^* , \quad (7.7)$$

where  $u_0^* \equiv \Gamma_0^{\mu\nu} a_\mu^* a_\nu^*$ .

These equations express the transformation properties of the structure constants under a translation (shift) of the coordinates. In particular if  $a_l^* = 0$  (as for the HT fixed point), one can see that since  $\Gamma_{00}^0 = 1$ , the transformation reduces to the identity. We will now study the transformation properties under changes of coordinates which will diagonalize the linear RG transformation matrix  $\mathcal{M}_i^j$ .

## B. Diagonalization of the linear RG

The diagonalization of the linear  $\mathcal{M}_i^j$  near the HT fixed point is quite simple because it is of the upper triangular form. The eigenvalues are just the diagonal terms. From Eq. (7.2), one sees that  $l$ th diagonal term is given as

$$\tilde{\lambda}_{(r)} = 2(c/4)^r . \quad (7.8)$$

This spectrum was obtained in Lemma 3.3 of Ref. [22] with a different method. This spectrum has a simple interpretation which will be discussed in subsection VII G. The upper diagonal form implies that the  $l - th$  right eigenvector has only its  $l$  first entries

non-zero. This means that if we truncate to  $a_{l_{max}}$ , we are simply truncating to a subspace spanned by the first  $l_{max}$  eigenvectors. This “stability” is due to the special relationship existing between the HT expansion and the polynomial truncation explained in section II.

On the other hand, the linearized map near the nontrivial fixed point does not have these simple properties. The eigenvalues may be determined numerically from a truncated version of the linearized matrix. With a large enough truncation, we can find a certain number of the eigenvalues to any desired precision. We find that there is one eigenvalue larger than 1, with all the rest less than 1. Though we do not have a simple formula for these eigenvalues, we know that they do shrink in size quickly. For instance the numerical values for  $c = 2^{1/3}$  are  $\lambda_1 = 1.42717\dots$ ,  $\lambda_2 = 0.85941\dots$ . A more complete list is given in Ref. [23].

Since  $\mathcal{M}$  is not a symmetric matrix the left and right eigenvector are distinct.

$$\mathcal{M}_l^i \psi_i^r = \lambda_{(r)} \psi_l^r \quad (7.9)$$

and

$$\phi_r^l \mathcal{M}_l^i = \lambda_{(r)} \phi_r^i . \quad (7.10)$$

The notation  $(r)$  means that there is no sum on  $r$ . Since all the eigenvalues are distinct, one can normalize the eigenvectors in such a way that

$$\phi_r^i \psi_i^{r'} = \delta_r^{r'} . \quad (7.11)$$

Similarly a completeness relation (decomposition of the identity) can be obtained by summing over  $r$ :

$$\phi_r^i \psi_j^r = \delta_j^i . \quad (7.12)$$

In numerical calculations, the relations of orthogonality and completeness provide a reliable way to check the accuracy of the calculations.

We can thus diagonalize the linearized RG:

$$\phi_r^l \mathcal{M}_l^i \psi_i^{r'} = \lambda_{(r)} \delta_r^{r'} . \quad (7.13)$$

If we start with the transformation expressed in the general form Eq. (7.3) but with  $a$  replaced by  $g$  to indicate that the fixed point is at the origin, as in the previous subsection, we can define a new set of coordinates  $d_{n,l}$ , such that

$$g_{n,l} = \psi_l^r d_{n,r} , \quad (7.14)$$

or, equivalently,

$$d_{n,r} = \phi_r^l g_{n,l} . \quad (7.15)$$

With these notations, all the structure constants transform according to the familiar rules of tensor analysis. Since  $\phi$  and  $\psi$  are inverse of each other, we can think of lower indices as covariant and upper indices as contravariant. As an example of transformation under Eq. (7.14), we have

$$\Gamma_p^{qr} \rightarrow \phi_p^{p'} \Gamma_{p'}^{q' r'} \psi_{q'}^q \psi_{r'}^r . \quad (7.16)$$

The other structure constants transform according to the same rules.

The eigenvectors are not determined uniquely even after normalizing. If  $\psi_i^r$  and  $\phi_r^i$  are components of normalized right and left eigenvectors, then  $\psi_i^r = \alpha_{(r)} \psi_i^r$  and  $\phi_r^i = \phi_r^i / \alpha_{(r)}$ , where  $\alpha_{(r)}$  is a constant, will work equally well. In the following, we will fix this ambiguity by requiring that the “other” fixed point be at  $(1, 1, \dots)$  in the new coordinates.

### C. Canonical Forms

In summary, we can choose a system of coordinate  $d_l$  where the unstable fixed point will be at the origin of the coordinate and the HT fixed point at  $(1, 1, \dots)$ , and such that the linear RG transformation is diagonal. In this system of coordinates, the RG transformation reads

$$d_{n+1,r} = \frac{\lambda_{(r)} d_{n,r} + \Delta_r^{pq} d_{n,p} d_{n,q}}{1 + \Lambda^p d_{n,p} + \Delta_0^{pq} d_{n,p} d_{n,q}} , \quad (7.17)$$

where the new structure constants are calculated from the original ones according to the transformation laws discussed in the previous two subsections.

Similarly, we can introduce new coordinates  $h_l$ , so that

$$a_{n,l} = \tilde{\psi}_l^r h_{n,r} , \quad (7.18)$$

and take the eigenvectors so that the unstable fixed point is at  $(1, 1, \dots)$  in the new system of coordinates. Note that the form of the eigenvectors guarantees that  $h_{n,l}$  is of order  $\beta^l$ . This can be seen by inverting Eq. (7.18) using the matrix of left eigenvectors. Due to the upper-diagonal form of the linear transformation, the second left eigenvector has its first entry equal to zero, the third its first two entries etc... . In this new system, the RG transformation reads

$$h_{n+1,r} = \frac{\tilde{\lambda}_{(r)} h_{n,r} + \tilde{\Delta}_r^{pq} h_{n,p} h_{n,q}}{1 + \tilde{\Lambda}^p h_{n,p} + \tilde{\Delta}_0^{pq} h_{n,p} h_{n,q}} . \quad (7.19)$$

#### D. Expansions in terms of the scaling fields

We would like to express the evolution of the canonical coordinates in terms of functions of the scaling fields:

$$d_{n,r} = \sum_{i_1, i_2, \dots} s_{r, i_1 i_2 \dots} y_{n,1}^{i_1} y_{n,2}^{i_2} \dots , \quad (7.20)$$

where the sums over the  $i$ 's run from 0 to infinity in each variable and  $y_{n,l} = \lambda_{(l)}^n y_{0,l}$ . In practice, we expand in terms of some finite number of the scaling fields, less than or equal to the number of  $d$  coordinates we have truncated to. Using the notation  $\mathbf{i} = (i_1, i_2 \dots)$  and the product symbol, we may rewrite the expansion as

$$d_{n,r} = \sum_{\mathbf{i}} s_{r, \mathbf{i}} \prod_m y_{n,m}^{i_m} \quad (7.21)$$

Using the transformation law for the scaling fields, we have

$$d_{n+1,r} = \sum_{\mathbf{i}} s_{r, \mathbf{i}} \prod_m (\lambda_{(m)} y_m)^{i_m} . \quad (7.22)$$

Each constant term,  $s_{r,0,0,\dots}$ , is zero, as the scaling fields vanish at the fixed point. From Eq. (7.17), we see that all but one of the linear terms are zero for each value of  $r$ . The remaining term is the one proportional to the  $r$ th scaling variable. We take these coefficients to be 1, so that the  $d_{n,r} \simeq y_{n,r}$  for small  $y_{n,r}$ . For the higher-order terms, we obtain the recursion

$$s_{r,\mathbf{i}} = \frac{\sum_{\mathbf{j}+\mathbf{k}=\mathbf{i}} (\Delta_r^{pq} s_{p,\mathbf{j}} s_{q,\mathbf{k}} - s_{r,\mathbf{j}} \prod_m \lambda_{(m)}^{j_m} \Lambda^p s_{p,\mathbf{k}}) - \sum_{\mathbf{j}+\mathbf{k}+\mathbf{l}=\mathbf{i}} s_{r,\mathbf{j}} \prod_m \lambda_{(m)}^{j_m} \Delta_0^{pq} s_{p,\mathbf{k}} s_{q,\mathbf{l}}}{\left( \prod_m \lambda_{(m)}^{i_m} - \lambda_r \right)}. \quad (7.23)$$

The calculation can be organized in such way that the r. h. s. of the equations are already known. This will be the case for instance if we proceed order by order in  $\sum_q i_q$ , the degree of non-linearity. This expansion may have small denominator problems. However, as discussed in the introduction, using numerical values of the eigenvalues as calculated in [23], we did not find spectacular cancellations between the two terms entering the denominator.

We can likewise expand each  $h_{n,r}$  in terms of scaling fields  $\tilde{y}_{n,1}, \tilde{y}_{n,2}, \dots$ . The derived recursions are identical in form to those derived above. From Eq. (7.8), one sees that the denominator will vanish for some equations. This question is discussed in [28] where it is shown that to all order relevant for the following calculation, a zero denominator always comes with a zero numerator.

### E. Expansion of the scaling fields

One can likewise find expansions of the scaling fields in terms of the canonical coordinates, by setting

$$y_{n,r} = \sum_{\mathbf{i}} u_{r,\mathbf{i}} \prod_m d_{n,m}^{i_m}, \quad (7.24)$$

and requiring that when  $\mathbf{d}_n$  is replaced by  $\mathbf{d}_{n+1}$ , the function is multiplied by  $\lambda_{(r)}$ . Since  $\mathbf{d}_{n+1}$  has a denominator, it needs to be expanded for instance in increasing order of non-linearity. A simple reasoning shows that exactly the same small denominators as in Eq. (7.23) will be present in these calculations. The same considerations applies for  $\tilde{y}$ .

It is in principle simple to obtain these expansions order by order in the degree of non-linearity, however there exists some practical limitations. For instance, if we want to calculate all the non-linear terms of order 10 in any of the variables, with  $l_{max}=30$ , we need to calculate and store  $30^{10} \sim 10^{15}$  numbers. In the next section, we show that one can organize these calculations more efficiently.

## F. The susceptibility

From Eqs. (2.6) and (7.18), we obtain

$$\chi_n = -(2/\beta)\tilde{\psi}_1^r h_{n,r} (2/c)^n . \quad (7.25)$$

For  $n$  large enough, the linear behavior applies and the  $h_{n,r}$  get multiplied by  $2(c/4)^r$  at each iteration. In the large  $n$  limit, only the  $r = 1$  term survives and consequently,

$$\chi = -(2/\beta)\tilde{\psi}_1^1 \lim_{n \rightarrow \infty} h_{n,1} (2/c)^n . \quad (7.26)$$

Using the same method as in the one-variable model, we can in the limit replace  $h_{n,1}$  by  $\tilde{y}_{n,1}$  and obtain

$$\chi = -(2/\beta)\tilde{\psi}_1^1 \tilde{y}_{0,1} . \quad (7.27)$$

This allows us to write

$$\chi = -(2/\beta)\tilde{\psi}_1^1 \Theta \tilde{y}_{0,1}^{-\gamma} , \quad (7.28)$$

where  $\gamma \equiv -\ln(\tilde{\lambda}_1)/\ln(\lambda_1)$  and  $\Theta$  the RG invariant

$$\Theta \equiv \tilde{y}_{0,1} \tilde{y}_{0,1}^\gamma = \tilde{y}_{n,1} \tilde{y}_{n,1}^\gamma . \quad (7.29)$$

For reference, in the case  $c = 2^{1/3}$  and with the normalization of the eigenvectors discussed above,  $\tilde{\psi}_1^1 \simeq -0.564$ .

## G. Higher moments

One can calculate the subtracted 2q-point function following the same procedure. As shown in [25,35], they can be expressed in terms of  $a_{q,n}$  and higher powers of the  $a_{n,l}$  with  $l < q$ . Following the procedure described above, these quantities can then reexpressed in terms of  $\tilde{y}$ . What is the leading term in this expansion?

By rescaling  $(-1)^q(2q)!a_{q,n}$  by  $(4/c)^n$  we obtain the average value of the  $2q$ -th power of the main spin (sum of the  $2^n$  spin variables  $\phi_x$ ). In the symmetric phase, this quantity scales like  $2^{qn}$  when  $n$  increases. However, the subtracted version of this quantity (which is generated by the free energy) is expected to scale like  $2^n$ . In other words,

$$a_{q,n} - (\text{subtractions}) \propto [2(c/4)^q]^n. \quad (7.30)$$

One clearly recognizes the spectrum of Eq. (7.8) . One then expects that the leading term is

$$a_{q,n} - (\text{subtractions}) \propto \tilde{y}_{n,q} . \quad (7.31)$$

In order to prove this conjecture by direct algebraic methods, one needs to show that the the non-linear terms which scale faster than  $\tilde{y}_{n,q}$  are canceled by the subtraction. For instance for the subtracted four-point function and  $c = 2^{1/3}$ ,  $\tilde{\lambda}_1^2 > \tilde{\lambda}_2$  and  $\tilde{\lambda}_1^3 > \tilde{\lambda}_2$ . We have checked that the corresponding terms  $(\tilde{y}_1)^2$  and  $(\tilde{y}_1)^3$  disappear with the subtraction. We have conducted similar checks for the 6 and 8 point functions [27] and found similar cancellations which still await a general explanation.

The practical calculation of the subtracted quantities is made difficult by the fact that as  $n$  increases, the “signal” becomes much smaller than the “background” (the unsubtracted part). This requires the use of adjustable precision arithmetic. In the following, we will only discuss the 2 point function (susceptibility).

## VIII. APPROXIMATIONS AND NUMERICAL IMPLEMENTATION

In this section, we show that it is possible to design approximations such that one can calculate the susceptibility using Eq. (7.29). For this purpose we have calculated an empirical series of  $a_{n,l}$  with  $c = 2^{1/3}$ , an initial Ising measure and  $\beta = \beta_c - 10^{-8}$ . Detail relevant for this calculations can be found in Refs. [25,23,37]. The calculations have been performed with  $l_{max} = 30$ , a value for which at the  $\beta$  considered, the errors due to the truncation are of the same order as those due to the numerical errors. These errors are small enough to allow a determination of the susceptibility with seven significant digits if we use double precision.

The empirical flow proceeds in two steps (see Fig. 1). First, the flow goes from the initial measure to close to the unstable fixed point. Second, the flow goes from close to the unstable fixed point to the HT fixed point. The first step depends on the choice of the initial measure and will not be discussed in full detail. As explained in the introduction, our main goal is to show that it is possible to construct nonlinear expansions which allow to describe accurately the second step. We now discuss the flow chronologically. In order to keep track of the chronological sequence, we postponed the technical discussion of the convergence of the series to section IX. In this section, these results are simply quoted.

Our choice of  $\beta$  (close to  $\beta_c$ ) means that we start near the stable manifold. After about 25 iterations, we start approaching the unstable fixed point and the linear behavior  $d_{n+1,l} \simeq \lambda_l d_n$  becomes a good approximation. During the next 20 iterations, the irrelevant variables die off at the linear rate and at the same time the flow moves away from the fixed point along the unstable direction, also at the linear rate. At  $n = 47$  we are in good approximation on the unstable manifold and  $d_{n,2}$  becomes proportional to  $d_{n,1}^2$ . In other words, the non-linear terms are taking over. At this point, we can approximate the  $d_{n,l}$  as functions of  $y_1$  *only*:  $d_{n,l} \simeq d_l(\lambda_1^n y_1, 0, 0, \dots)$ . This approximation is consistent in the sense that if  $y_2 = 0$  at  $n = 0$  then it is also the case for all positive  $n$ .

We have calculated  $d_l(y_1, 0, 0, \dots)$  up to order 80 in  $y_1$  using Eq. (7.23). There cannot

be any small denominators in this restricted case. We have then inverted  $d_1$ , now a function of  $y_1$  only, to obtain  $y_1(d_1)$ . Given the empirical  $d_{n,1}$  we then calculated the approximate  $y_{n,1}$  and then used the other functions  $d_l(y_1)$  (with  $l \geq 2$ ) calculated before to “predict”  $d_{n,l}$ . Comparison with the actual numbers were good in a restricted range. For  $n = 49$ , the relative errors were less than a percent. They kept decreasing to less than one part in 10,000 for  $n = 54$  and then increased again. It will be shown in section IX that this corresponds to the fact that when  $y_1$  becomes too large (a value of approximately 3.7 first exceeded at  $n = 57$ ), the series expansion of  $d_1$  diverges, unlike the one-variable model for which  $d(y)$  is analytical. It will also be shown later that the quality of the approximation between  $n = 45$  and  $n = 55$  can be improved by by treating  $y_2$  perturbatively.

Near  $n = 55$ , the presence of the HT fixed point starts dominating the flow but we are still far away from the linear regime. We have taken these non-linear effects in  $\tilde{y}_1(\mathbf{h})$  by calculating it up to order 11 in  $\beta$ . This is a multi-variable expansion. Recalling the discussion about the HT expansion in section II and the properties of the eigenvectors of the linearized RG transformation about the HT fixed point, we can count the number of terms at each order in  $\beta$ . At order two, we have  $h_1^2$  and  $h_2$ , but since the linear transformation is diagonalized,  $h_2$  will only appear in  $\tilde{y}_2(\mathbf{h})$ . At order three, we have  $h_1^3$ ,  $h_2h_1$  and not  $h_3$ . It is easy to see that at order  $l$ , one has  $p(l) - 1$  terms, where  $p(l)$  is the number of partitions of  $l$ . It has been known from the work of Hardy and Ramanujan that

$$p(l) \sim \frac{\exp(\pi\sqrt{2l/3})}{4\sqrt{3}l} . \quad (8.1)$$

It seems thus difficult to get very high order in this expansion. In order to fix the ideas, there are 41 terms at order 11, 489 at order 20 and 13,848,649 at order 80.

As we will explain in section IX, the expansion up to order 11 has a sufficient accuracy to be used starting at  $n = 55$ . It also provides optimal (given our use of double precision) results for  $n \geq 60$ . As  $n$  increases beyond 60, one can see the effect of each order disappear one after the other. Finally, the linear behavior becomes optimal near  $n = 130$ . This concludes our chronological discussion. The main point made was that there exists a region

in the crossover where both expansions are valid. We now proceed to justify empirically the claims made above.

## IX. LARGE-ORDER BEHAVIOR FOR THE HM

### A. $y_1(d_1)$

The behavior of  $y_1(d_1)$  obtained by the procedure described above, has been studied following the same methods as for the one-variable model. In order to provide a comparison, we have calculated the same quantities for the one-variable model with  $\lambda = 1.2573$ . In the following, we call this model the “simplified model” (SM). For this special value, the critical exponents  $\gamma$  of the two models coincide with five significant digits. We have good evidence that both series have a radius of convergence 1 as indicated by the extrapolated ratio defined in Eq. (2.12) reaching 1 at an expected rate (Fig. 16).

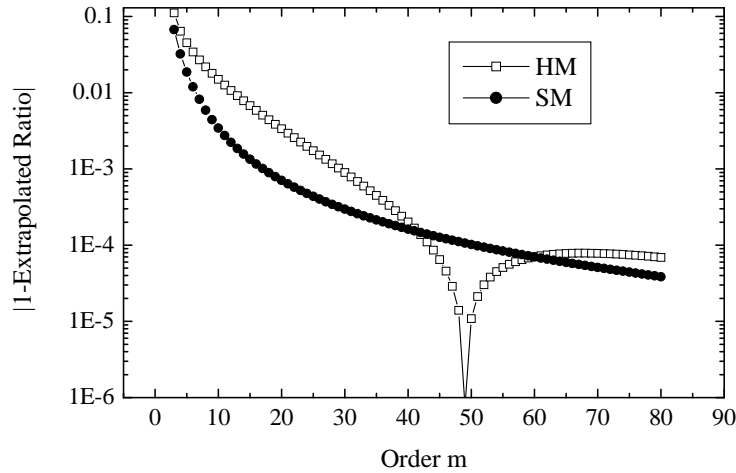


FIG. 16. The absolute value of the difference between the extrapolated ratio and 1 for the HM (empty boxes) and the SM (full circles), as a function of the order.

Similarly, their extrapolated slopes seem to converge to the same value  $1/\gamma - 1 \simeq -0.23026\dots$  as shown in Fig. 17.

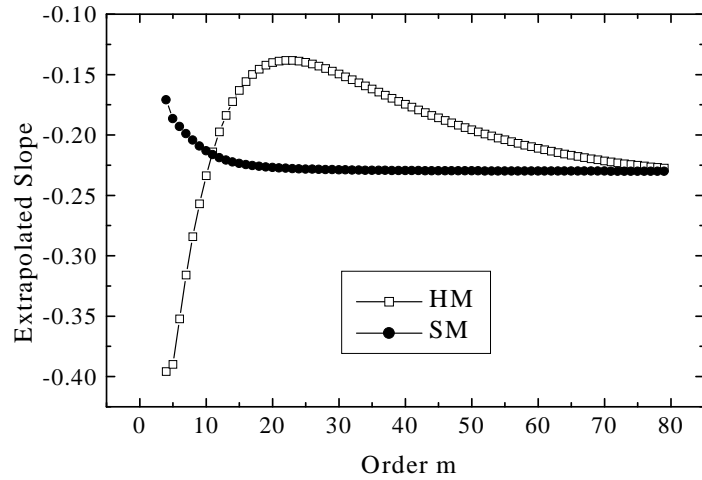


FIG. 17. The extrapolated slope  $\hat{S}_m$  for the HM (empty boxes) and the SM (full circles) as a function of the order .

In conclusion, the function  $y(d)$  for the SM is a reasonably good model to guess the asymptotic behavior of  $y_1(d_1)$ .

### B. $d_1(y_1)$

The situation is different for the inverse function  $d_1(y_1)$ . A first look at the differences is given in Fig. 18.

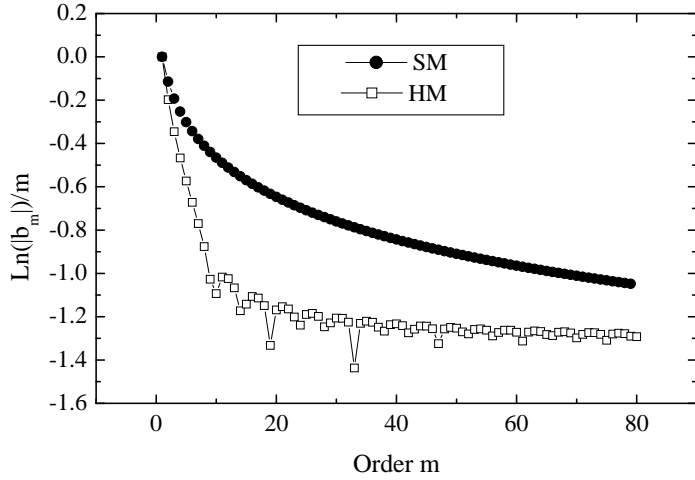


FIG. 18. Logarithm of the absolute value of the coefficients of the expansion of  $d_1(y_1)$  divided by the order, for the HM (empty boxes) and the SM (circles).

The quantity plotted in this figure will be used to discriminate between a finite and an infinite radius of convergence. If  $|b_m| \sim R^{-m}$  as for a radius of convergence  $R$ , then we have  $\ln(|b_m|)/m \sim -\ln(R) + A/m$  for some constant  $A$ . On the other hand, if  $|b_m| \sim (m!)^{-\alpha}$  as for an infinite radius of convergence, then we have  $\ln(|b_m|)/m \sim -\alpha(\ln(m) - 1)$ . In the following, we will compare fits of the form  $A_1 + A_2/m$  and  $B_1 \ln(m) + B_2$ .

We first consider the case of SM, where according to our study in section V, expect an infinite radius of convergence. This possibility is highly favored as shown in Fig. 19.

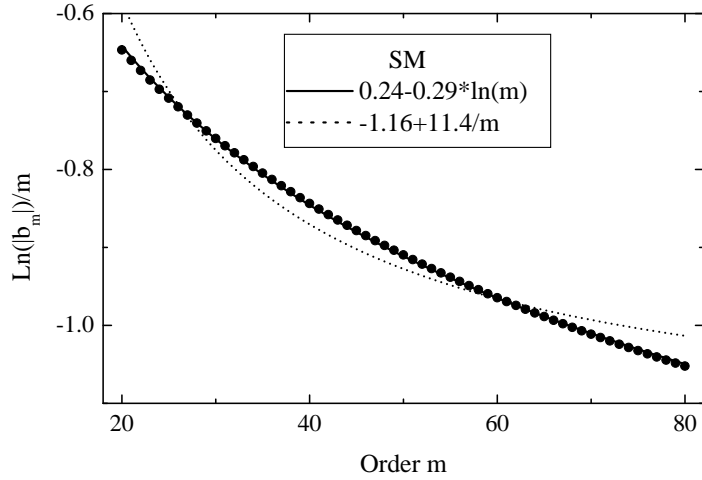


FIG. 19. Comparison of fits of the form  $A_1 + A_2/m$  (dots) and  $B_1\ln(m) + B_2$  (solid line) with the data provided in Fig. 18 for the SM (circles).

One sees clearly that the solid line is a much better fit. The chi-square for the solid line fit is 200 times smaller. In addition  $B_1 \simeq -B_2$  as expected. In conclusion, this analysis confirms the ratio analysis done previously and favors strongly the infinite radius of convergence possibility.

The analysis for the HM is more delicate. One observes periodic “dips” in Fig. 18 which make the ratio analysis almost impossible. We have thus only considered, the “upper envelope” by removing the dips from Fig. 18. The fit represents an upper bound rather than the actual coefficients. The fits of the upper envelope are shown in Fig. 20.

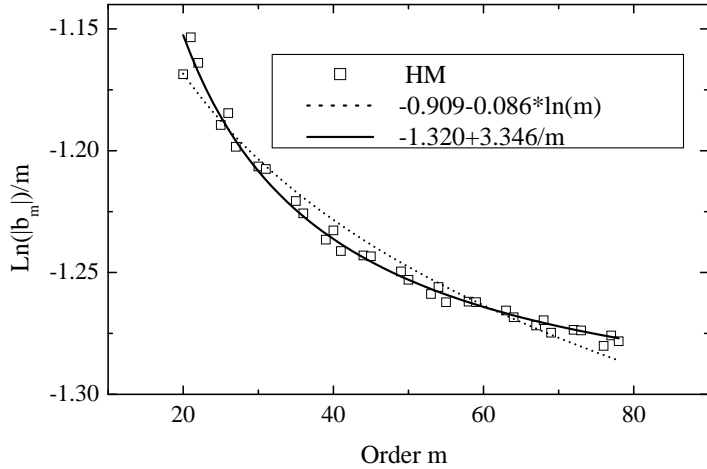


FIG. 20. Comparison of fits of the form  $A_1 + A_2/m$  (solid line) and  $B_1\ln(m) + B_2$  (dots) with selected points of the data in Fig. 18 for the HM (boxes).

The possibility of a finite radius of convergence is slightly favored, the chi-square being 0.4 of the one for the other possibility. Also, the second fit does not have the  $B_1 \simeq -B_2$  property. From  $A_1 \simeq -1.32$ , we estimate that the radius of convergence is about 3.7. This means that if we want to write some analytical formula for the flows by first calculating the initial values of the scaling fields and then calculating  $\mathbf{d}$  at successive iterations by using their expression in terms of the scaling fields, we will have to switch variables in the crossover region.

### C. $\tilde{y}_1(\mathbf{h})$

Up to now we have only considered functions of one variable and their inverse. We have shown that the leading singularity of these functions can be analyzed reliably. It is not difficult to show that the information related to the convergence of the series associated with a scaling field, and the way it actually scales are consistent. This will be shown explicitly for  $y_1(d_1)$  in subsection IX D. Such a simple analysis is not possible near the HT fixed point of the HM, because we as explained in section VIII, the approach of the HT fixed point is intrinsically a multivariable problem. For this reason, the calculation of  $D_n$  that tests the

quality of scaling will be our main tool of analysis in this subsection.

In the following, we limit the discussion to  $\tilde{y}_1(\mathbf{h})$  which enters in the susceptibility. We have calculated  $\tilde{y}_1(\mathbf{h})$  in terms of 11 variables, up to order 11 in  $\beta$ . As in section V, we will use an empirical series  $a_{n,l}$ , calculate the corresponding  $h_{n,l}$  and plug them in the scaling fields and check the scaling properties. This empirical series was calculated with an initial Ising measure and  $\beta = \beta_c - 10^{-8}$  (see Ref. [23]). Again we define a quantity  $D_n$  as in Eq. (6.11) which is very small when we have good scaling and increases when the approximation breaks down. The results are shown in Fig. 21 for successive orders in  $\beta$ .

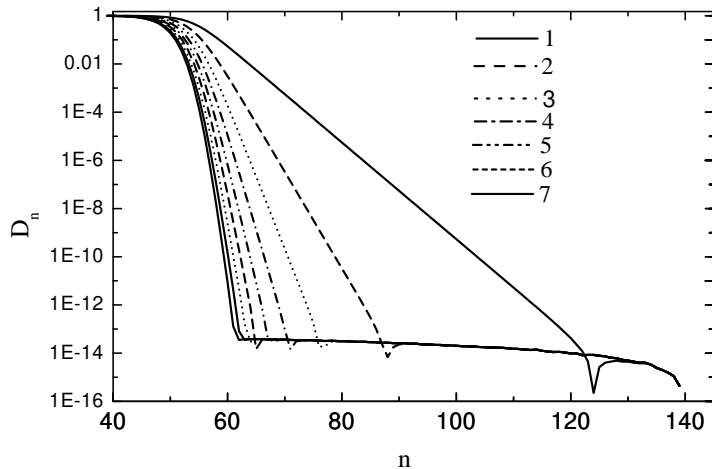


FIG. 21. The quantity  $D_n$  defined in Eq. (6.11) for expansions of  $\tilde{y}_1$  in  $\beta$ , at order 1 (solid line), 2 (dashes), 3 (dots), etc... for each iteration  $n$ .

The solid line on the right is the linear approximation. It becomes optimal near  $n = 130$ . The next line (dashes) is the second order in  $\beta$  expansion. It becomes optimal near  $n = 90$ . Each next order gets closer and closer to be optimal near  $n = 60$ . The last curve on the left is the order 9 approximation. It is hard to resolve the next two approximations on this graph.

The asymptotic value is stabilized with 16 digits and one may wonder why we get only scaling with 14 or 15 digits in Fig. 21. The reason is that we use empirical data and that

numerical errors can add coherently as explained in Ref. [37]. This can be seen directly by considering the difference between two successive values of  $D_n$  as shown in Fig. 22.

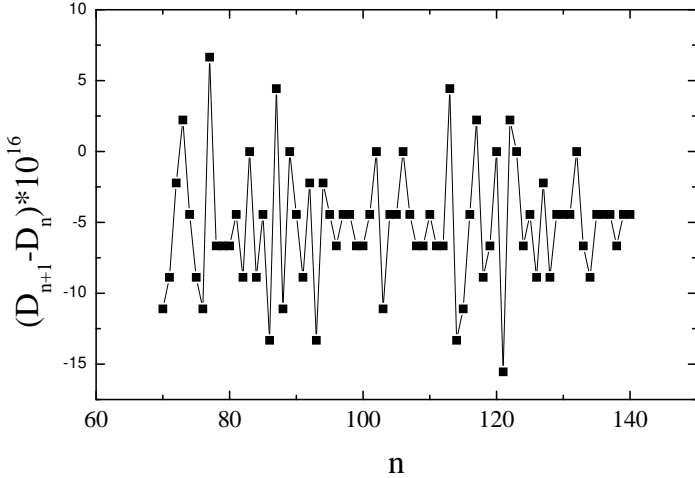


FIG. 22. Difference between two successive  $D_n$  in  $10^{-16}$  units.

One sees that the numerical errors at each step tend to be negative more often than positive, and consequently there is a small “drift” which affects the last digits.

#### D. Tests of scaling

We can now look at the  $D_n$  defined as in Eq. (6.11) for  $y_1$  and  $\tilde{y}_1$  together in Fig. 23. If we use an expansion of order 5 in  $\beta$  for  $\tilde{y}$  and of order 10 in  $d_1$  for  $y_1$ , we can get scaling within a few percent for both variables at  $n = 54$ . We can go below 1 part in 1000, with an expansion of order 11 in  $\beta$  and order 80 in  $d_1$ . At this point, the main problem is that the effects of the subleading correction makes the scaling properties *worse* when  $n \leq 57$  and  $n$  decreases. One can improve the scaling properties by taking the effects of  $y_2$  into account. A detailed study shows that one can estimate the subleading effects between  $n = 40$  and  $n = 45$ . One finds that

$$\frac{y_1(d_{n,1})}{\lambda_1^n} \simeq 7.2778 \times 10^{-9} + 3.2 \times 10^{-9} \times \lambda_2^n \quad (9.1)$$

It is thus possible to get a function scaling better by subtracting these correction. This improve the scaling properties by almost one order of magnitude near  $n = 54$  and by almost two order of magnitude near  $n = 45$ . It is likely that our approximation of having a single scaling variable can be corrected order by order in  $y_2$ ,  $y_3$  etc... .

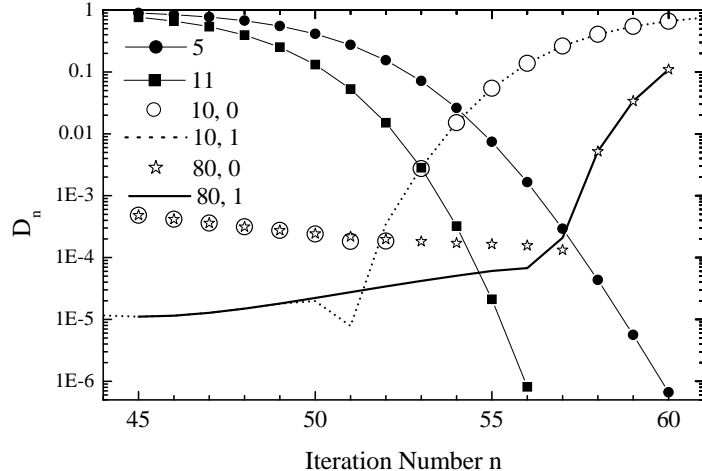


FIG. 23. Values of  $D_n$  for  $\tilde{y}_1$  up to order 5 in  $\beta$  (filled circle) and 11 (filled boxes), and for  $y_1$  up to order 10 in  $d_1$  (empty circles) and with first order corrections in  $y_2$  (dots), and up to order 80 in  $d_1$  (empty stars) and with first order corrections in  $y_2$  (solid line).

Note that the values of  $D_n$  for  $y_1$  when  $n$  becomes large are compatible with the analysis of subsection IX A showing that  $y_1(d_1)$  has a leading singularity of the form  $A(1 - d_1)^{-1/\gamma}$ . Calculating the difference between the leading singularity and its expansion to a finite order, for a fixed value of  $d_1$ , we obtain very accurate estimates of  $D_n$ . To give a concrete example, at  $n = 60$  the effects of the subleading  $y_2$  are negligible and our estimated value of  $d_1$  is 0.978. Using the expansion up to order 80 for the leading singularity, we obtain a relative error of 0.1114 while the empirical value of  $D_{60}$  is 0.1095.

## X. CONCLUSIONS

We have shown in two examples that the susceptibility can be expressed in terms of the scaling fields corresponding to the two fixed points governing the HT flows. We have given convincing numerical evidence that the expansions of these scaling fields scale properly in overlapping domains. Several interesting questions remain to be discussed.

As emphasized in the introduction, all the results presented here are numerical. Our study suggests that several analytical investigations should be conducted. In particular, in the construction of the scaling variables near the HT fixed point, two types of “miraculous” cancellations (for the small denominators and for some nonlinear terms in the subtracted  $2q$ -point functions) still await a general explanation.

We have not discussed in detail the initial approach of the unstable fixed point. We have just shown that it can in principle be incorporated by calculating the subleading corrections in  $y_2$ ,  $y_3$  etc... This study depends on the details of the initial measure. A particularly interesting set of initial measures are the Landau-Ginzburg models in the vicinity of the Gaussian fixed point. We can use the usual perturbation theory in the quartic (or higher orders) coupling constant to construct the scaling fields associated with the Gaussian fixed point following the procedure described above, and interpolate between the Gaussian fixed point and the unstable fixed point.

The study of the initial flow is also crucial to be able to express the scaling fields in terms of the “real fields” such as the reduced temperature. This would allow a detailed comparison with the predictions of scaling hypotheses found in the literature [32,33,31]. Another interesting question that could be addressed within this context is the crossover from classical to critical behavior [6,8–12]. These questions are under investigation [27].

It seems clear from the discussion of subsection VII G that not only the susceptibility but also the higher derivatives of the free energy have a simple expression in terms of the HT scaling fields. If this can actually be proven and if we can solve the problems of the initial flows, then we should be in position to solve the central problem in field theory, namely to

give analytical expressions for the renormalized quantities in terms of the bare ones.

The hierarchical approximation used in this article has allowed us to calculate large order expansions for the scaling fields. The fact that the general ideas advocated have worked properly means that one should now attempt to apply them to nearest neighbor models where similar calculations would be more time consuming. The examples we have in mind are asymptotically free theory such as the  $O(N)$  spin models in two dimensions or lattice gauge theory in four dimensions. In both cases, there exists some advanced technology for the weak and strong coupling expansions and the question of the interpolation as been studied with the Monte Carlo method [5,7].

#### ACKNOWLEDGMENTS

This research was supported in part by the Department of Energy under Contract No. FG02-91ER40664. Y. M. thanks the Aspen Center for Physics for its hospitality in Summer 1999, where discussions with P. de Forcrand motivated the completion of this work and in Summer 2000 while part of this manuscript was written.

---

- [1] V. Arnold, *Geometrical Methods in the Theory of Ordinary Differential Equations* (Springer-Verlag, New York, 1988).
- [2] H. Poincaré, *Les Methodes Nouvelles de la Mecanique Celeste* (Gauthier-Villars, Paris, 1892).
- [3] F. Wegner, Phys. Rev. B **3**, 4529 (1972).
- [4] J. Cardy, *Scaling and Renormalization in Statistical Physics* (Cambridge University Press, Cambridge, 1996).
- [5] A. Gonzalez-Arroyo and M. Okawa, Phys. Rev. D **35**, 672 (1987).
- [6] E. Luijten and K. Binder, Phys. Rev. E **58**, R4060 (1998).

- [7] P. de Forcrand et al., Nucl. Phys. B **577**, 263 (2000).
- [8] C. Bagnuls and C. Bervillier, Phys. Rev. **B32**, 7209 (1985).
- [9] A. Pelissetto, P. Rossi, and E. Vicari, Phys. Rev. **E58**, 7146 (1998).
- [10] A. Pelissetto, P. Rossi, and E. Vicari, Nucl. Phys. **B554**, 552 (1999).
- [11] A. Pelissetto and E. Vicari, Critical phenomena and renormalization-group theory, 2000, cond-mat/0012164.
- [12] S. Caracciolo *et al.*, Crossover phenomena in spin models with medium-range interactions and self-avoiding walks with medium-range jumps, 2001, cond-mat/0105160.
- [13] J. Gaite and D. O'Connor, Phys. Rev. D **54**, 5163 (1996).
- [14] B. Nickel, in *Phase Transitions, Cargese 1980*, edited by M. Levy, J. L. Guillou, and J. Zinn-Justin (Plenum Press, New York, 1982).
- [15] M. Campostrini, J. Stat. Phys. **103**, 369 (2001).
- [16] Y. Meurice, G. Ordaz, and V. G. J. Rodgers, Phys. Rev. Lett. **75**, 4555 (1995).
- [17] Y. Meurice, S. Niermann, and G. Ordaz, J. Stat. Phys. **87**, 363 (1997).
- [18] K. Wilson, Phys. Rev. B. **4**, 3185 (1971).
- [19] F. Dyson, Comm. Math. Phys. **12**, 91 (1969).
- [20] G. Baker, Phys. Rev. B **5**, 2622 (1972).
- [21] P. Bleher and Y. Sinai, Comm. Math. Phys. **45**, 247 (1975).
- [22] P. Collet and J. Eckmann, *A Renormalization Group Analysis of the Hierarchical Model in Statistical Mechanics* (Springer-Verlag, Berlin, 1978).
- [23] J. Godina, Y. Meurice, and M. Oktay, Phys. Rev. D **59**, 096002 (1999).
- [24] H. Koch and P. Wittwer, Math. Phys. Electr. Jour. **1**, Paper 6 (1995).

- [25] J. Godina, Y. Meurice, M. Oktay, and S. Niermann, Phys. Rev. D **57**, 6326 (1998).
- [26] J. Godina, Y. Meurice, and M. Oktay, Phys. Rev. D **57**, R6581 (1998).
- [27] L. Li and Y. Meurice, in preparation.
- [28] Y. Meurice, Phys. Rev. E **63**, 055101(R) (2001).
- [29] Y. Meurice and S. Niermann, Phys. Rev. E **60**, 2612 (1999).
- [30] T. Niemeijer and J. van Leeuwen, in *Phase Transitions and Critical Phenomena, vol. 6*, edited by C. Domb and M. Green (Academic Press, New York, 1976).
- [31] A. Aharony and M. Fisher, Phys. Rev. B **27**, 4394 (1983).
- [32] A. Aharony and G. Ahlers, Phys. Rev. Lett. **44**, 782 (1980).
- [33] M. Chang and A. Houghton, Phys. Rev. Lett. **44**, 785 (1980).
- [34] Y. Meurice and B. Oktay, in preparation.
- [35] J. J. Godina, Y. Meurice, and M. Oktay, Phys. Rev. D **61**, 114509 (2000).
- [36] P. Collet and J.-P. Eckmann, *Iterated maps of the interval as dynamical systems* (Birkhauser, Boston, 1980).
- [37] Y. Meurice and B. Oktay, Phys. Rev. D **63**, 016005 (2001).